Summary

This thesis has investigated the feasibility of using end-drawn stainless steel fiber with diameter of 8μm to make fiber reinforced polymer composite produced through filament winding method. The main objective for this thesis has been to investigated the hybridisation effect between steel- and carbon fiber when used in fiber reinforced polymer composite pressure vessels. Mechanical- and elastic properties has been obtained by experimental tests and evaluated by analytical methods.

Two different composite products have been produced through filament winding method for this study; ring specimens and pressure vessels. The ring specimens were produced with three different fiber material configuration; Steel Fiber Reinforced Polymer (SFRP), Carbon Fiber Reinforced Polymer (CFRP), and a hybrid between SFRP and CFRP. The pressure vessel were produced with $[90°_{2C}/\pm15°_{2C}/90°_{2S}]$ layup. Burn-off test and microscopy image analysis were used to determine fiber volume fraction of the composites produced, and used for calculation of elastic properties. Void count, bonding between steel and carbon fiber layers, and ply thickness has also been assessed.

Split-disk test were conducted on the ring specimens and mechanical properties compared between each other. The results from the testing showed that the desired strain-to-failure value of the steel fiber in dry form did not transfer when used as fiber reinforcement in epoxy matrix. The hybridization of steel- and carbon fiber was not successful in improving the strain-to-failure of CFRP, it was however able to increase the tensile strength of the hybrid ring samples when compared with the SFRP ring samples. The impact test conducted on the pressure vessel produced in the study showed improvement in impact resilience when using SFRP as outer hoop layers in the composite overwrap of the pressure vessel compared to using CFRP composite overwrap. The SFRP hoop layers showed to have a more ductile impact imprint and less fiber failure from the impact than the CFRP hoop layers.

Sammendrag

Denne oppgaven har undersøkt muligheten for bruk av ende-trukket rustfritt stålfiber med diameter på 8 μm for å produsere fiberforsterket polymerkompositt produsert gjennom filamentviklingsmetode. Hovedformlet med denne oppgaven har vært å undersøke hybridiseringseffekten mellom stål- og karbonfiber når det brukes i fiberforsterket polymer kompositt trykkbeholdere. Mekaniske og elastiske egenskaper har blitt evaluert ved eksperimentelle tester og analytiske metoder har blitt brukt til å sammenligne resultater.

To forskjellige sammensatte produkter har blitt produsert gjennom filamentviklingsmetode for denne studien; ringprøver og trykkbeholdere. Ringeprøver ble produsert med tre forskjellige fibermaterialekonfigurasjoner; SFRP, CFRP, og en hybrid mellom SFRP og CFRP. Trykkbeholderne ble produsert med $[90°_{2C}/\pm15°_{2C}/90°_{2S}]$ layup. Avbrenningstest og mikroskopi-bildeanalyse ble brukt for å bestemme fibervolumfraksjonen av de produserte komposittene og benyttet til beregning av elastiske egenskaper. Tomrom andel, binding mellom stål og karbonfiber lagene, og lagtykkelse har ogs blitt vurdert.

Split-disk test ble utført på ringprver og mekaniske egenskaper sammenlignet mellom hverandre. Resultatene fra testen viste at den ønskede strekk-til-sviktverdien av stlfiberen i tørr form ikke ble overfrt når den ble brukt som fiberforsterkning i epoksymatrise. Hybridiseringen av stål- og karbonfiber lyktes ikke i forbedre strekk-til-brudd av CFRP kompositt, men det var imidlertid i stand til øke strekkfastheten til hybridprøvene sammenlignet med SFRP ringprøver. Dropptesten som ble utført p trykkbeholderen som ble produsert i studiet viste forbedring i støt motstand ved bruk av SFRP som ytre hoop lag i komposittomfanget av trykkbeholderen sammenlignet med bruk av CFRP komposittomslag.

Table of Contents

List of Tables

List of Figures

Symbols & Acronyms

Symbols

$E_{1,f}$	Elastic modulus in longitudinal direction of the fiber material.
E_2	Elastic modulus in transverse direction.
E_m	Elastic modulus of matrix.
G_{12}	Shear modulus in-plane.
V_f	Volume fraction of fiber in composite.
ν_{12}	Poisson's ratio in-plane.
ρ	Density of the composite.
σ_a	Helical/axial stress.
σ_h	Hoop stress.
r_i	Inner radius.
p	Internal pressure.
t	Thickness of the laminate.

Acronyms

CFRP	Carbon Fiber Reinforced Polymer.
CLT	Classical Laminate Theory.
CNG	Compressed Natural Gas.
COPV	Composite Overwrapped Pressure Vessel.
FEA	Finite Element Analysis.
FEM	Finite Element Method.
HDPE	High-Density Polyethylene.
NDT	Non Destructive Testing.
RVE	Representative Volume Element.

SFRP   Steel Fiber Reinforced Polymer.
UTS   Ultimate Tensile Stress.

Chapter 1

Introduction

1.1 Problem Statement

Composite pressure vessels made out of glass or carbon fibers with polymeric matrices are being widely used today. As the benzene/diesel demand are replaced by natural gas and eventually hydrogen, the demand for adequate solutions of pressure vessels will increase. The utilization of metallic fiber reinforced polymers is in its infant state as there exist little to no research on metallic fiber reinforced polymer pressure vessels. The majority of the current scientific research on metallic fibers is constricted to unidirectional continuous steel fibers in the application of mats and cross-ply laminates, but are lacking when it comes to curved structures such as filament wound composite pressure vessels. This study will investigate the feasibility of introducing steel fiber in high-pressure gas storage. The advantage of such vessels is suggested to improve impact resilience, safer rapture mode and lower cost. Different lay-ups with hybridization of steel and carbon fiber to reinforce composite overwrapped pressure vessel shall be produced through filament winding method. The properties of the different configurations shall be investigated, and experimental failure tests will be conducted. Elastic properties from both numerical calculations and analytical analysis will be compared with experimental results.

1.2 Literature Review

The current research that contains utilization of metallic fibers to reinforce polymers are limited. The research that is conducted on metallic fibers in continuous form is in a strong degree limited to stainless steel fiber. Stainless steel fiber is not new to being used as reinforcement. It has been used for decades in concrete, cut resilient fabrics, and conveyor

belts etc. In recent year, there have been more research on using steel fiber as reinforcement in polymer composite.

Callens [5] investigated utilization of annealed stainless steel fibers in composite applications. He found that the steel fiber increased the composite stiffness and strain-to-failure with 10 and 5 times compared to glass- and carbon fiber. The investigation also studied steel fiber hybrids with glass- and carbon fiber. This resulted in a composite with increased strength and the abrupt fiber failure that can often be found in glass- and carbon fiber was not present. Despite the increases in properties, the strain-to-failure was eminently lower than in the pure steel fiber composite.

Tran [6] used non-annealed steel fiber to reinforce polymer composite pipes by filament winding steel fiber with $\pm 55°$ layup. He found that using steel fiber to reinforce the polymer gave a much higher strain-to-failure than what was found using unidirectional carbon fiber, as much as three times greater. The research also showed an increase in the combined stiffness of the composite with steel fiber.

Callens et al. [7] researched the effect of three different weave architecture on the tensile and impact behaviour of ductile SFRP composites. He found that all the weave architectures had the same strain-to-failure, even though they had different crimp. The result also showed that the composite with the basket weave showed a distinct reduction in stiffness and yield stress compared to the two other weaves. The basket weave was observed to have out of plane deformations during tensile strength test. The impact testing of the composite weaves showed that the high ductility of the stainless steel fibers correlates with exceptional impact performance.

1.3   Current Market

The demand for composite reinforced pressure vessels to store high pressure gasses is growing, and has been growing the last decades, in a rapid pace. Glass- and carbon fiber reinforced composite overwraped pressure vessels produced by filament winding was originally developed for the military and has been eminently used for oxygen and gas storage in the aerospace-industry due to the need for high stiffness-to-weight ratio. Later it has been introduced in the civilian market in various applications such as breathing apparatuses used by fire-fighters and scuba divers. The primary end-marked for the advanced composite reinforced pressure vessels are in tank- and bulk transportation of Compressed Natural Gas (CNG), and fuel storage for emission friendly transportation vehicles that uses CNG and Hydrogen instead of benzene or diesel. The demand for alternative fuel for transportation is ever rising. This has been made possible due to extraction of shale reserves that drives the price of CNG and hydrogen down. The increase of emission regulations also contributes to driving the price up for benzene and diesel transportation. The regulations and the consumer shift from Benzene and diesel to CNG and hydrogen as the future choice of fuel helps driving the market for fiber reinforced composites forward [8]. To successfully fulfill the growing demand for proficient and effective pressure vessels, the cost of these products needs to be driven down. As a study conducted by Hua, T.Q et al.

[9] on hydrogen fuel tanks in transportation vehicles, shows that carbon fiber reinforced composite vessels contributes to >70% of the total system cost.

1.4   Material Selection

Prior to the beginning of this thesis, as a preparation project, a material investigation of the current markets metallic fibers were completed. The material choice for this thesis were done from the finding of that project. Since the metallic fibers are going to be used for filament winding, the fibers need to be bundled continuous fibers. Steel fibers provides a combination of high stiffness (Ī93GPa) and high strain to failure, up to 20%. These qualities makes steel unlike most of the natural fibers and other metallic fibers. Steel makes also a favourable option due to its low price in its raw form. Since steel is susceptible to corrosion, there is a need of adding alloying elements such as chromium, nickel, and molybdenum. The alloying elements that is needed to make the steel fiber corrosion resistance is going to bring the cost up. It also limits the amount of carbon content added to the alloy. Although carbon is an effective alloy element to increase the strength of steel, it also decrease the ductility and hinder corrosion resistance by promoting the formation of precipitates [10]. This means that the tensile strength of the steel fiber is going to be lower than what is possible for high carbon steel. The cost for raw steel is 1$/kg. When adding the price of alloying materials and production cost of the drawing process, the cost goes up to roughly 2.5$/kg. Compared to carbon fiber, which costs 15-20 $/kg, this is a relatively low cost for fiber material. When comparing the density of steel (7.9 kg/m^3) and carbon (1.8 kg/m^3), the steel is around 4 times greater than carbon. Adding to this, looking at the cost-per-strength between steel and carbon, it is clear that carbon fiber is far superior to steel fiber when comparing strength-to-weight. AISI 302A stainless steel fiber were selected as a prominent candidate to use for this thesis. 302A steel fiber provides a similar stiffness (200 GPa) when compared with carbon fiber (230GPa), the strain-to-failure of 302A (4-5%) is higher than carbon fiber (1.8%), and it has the highest tensile strength (950 MPa) of all the other steel fibers that are available in continuous form in the current market.

Material	Tensile strength [MPa]	Elastic modulus [GPa]	Density [g/cm^3]	Poisson's ratio
AISI 302A	950	200	7.9	0.3
AISI 316L	660	193	7.9	0.3
Aluminium	70	69	2.8	0.32
Titanium	900	115	4.5	0.34
Copper	220	117	9.0	0.33
Manganese	496	159	7.4	0.33
Glass fiber	2400	70	2.6	0.3
Carbon fiber	4400	230	1.8	0.3

Table 1.1: Material properties of various materials considered [1]

Chapter 2

Basic Theory

2.1 Steel Fiber

Glass- and carbon fiber is the current market's dominant material choice when it comes to pressure vessels. They have replaced the usage of solid steel vessels due to their light weight and cost efficient properties, while still have an impressive strength.

The steel fiber are produced by a production process called bundle drawing. The process begins by cladding stainless steel wires with a sacrificial alloy, usually copper or iron. Cladding the steel wire is done using a rolling mill, and produces what is called composite wire. This helps with keeping all the individual wires separate from each other. When the cladding of the steel wire is done, the composite wire is annealed to increase machinability so it can be drawn. The wire drawing process pulls the composite wire through dies, which is commonly made out of diamond or carbide. By repeating this drawing process, the diameter of the composite wire is reducing each time is passes a die. The initial drawing allows for more aggressive reduction of the cross section than later in the process, as the wire gets hardened each time it passes a die. Each die typically reduces the cross section area by 15%, and elongates the wire by the same amount.

The bundle drawing process takes up to thousands of composite wires, or filaments, bundled together and goes through a second cladding as a "tube" (Figure 2.1). Then the bundle is passed through the dies again to further decrease the diameter of the filaments. Once the desired size is achieved, the cladding alloy is removed by either chemical or electrochemical leaching. Since stainless steel allows for high deformation between annealing treatments, the number of annealing for the whole drawing process can be reduced.

The bundle drawing process allows for the stainless steel fiber to be produced as continuous fiber from a single simultaneous drawing operation. The bundled fibers are formed together in tows which is wounded on spools with lengths up to several kilometers. Usu-

ally, at least for glass and carbon fiber, the fibers are covered with a thin coating called sizing. This is to prevent the fibers to be damaged when they are brushing against each other and equipment during processing. The sizing protects the fibers by serving as a lubricant and anti-static agent. It also works as a coupling agent that promotes the bonding with the matrix when used as a reinforcement in composites [11]. The steel fibers used in this thesis does not have any size, as reported from the manufacturer this is not necessary for the steel fiber due to good bonding with epoxy. When the steel fiber is finished with the bundle drawing they are spun onto spools in tows, which are commonly expressed in terms of a tow count value, K. The K-value expresses the number of steel filaments the steel fiber tow contains, and typically ranges from 1K to 36K where K is in thousands. With recent developments the last decade, the technology of bundle drawing allows for the production of fibers with diameter of 200nm.
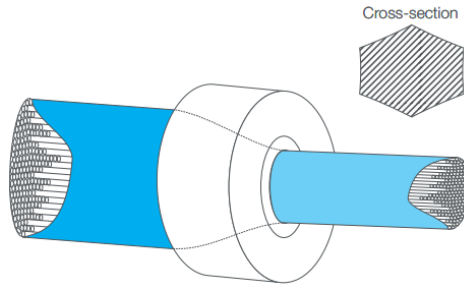
Figure 2.1: Bundle drawing.

	Material		
Mechanical Properties	SS 302 A	SS 316L	EPIKOTE MGS RIMR 135 Epoxy Resin
Elastic modulus [GPa]	200	193	3.2
Tensile strength, σ_{UTS} [MPa]	950	680	65
Strain-to-failure [%]	3-5	19	12
Poisson's ratio	0.3	0.3	0.35
Density [g/cm^3]	8	8	1.2

Table 2.1: Mechanical properties of stainless steel with $d = 8\mu m$ and epoxy resin. [2]

	Alloy Composition, wt%							
Material	C	P	Ni	Mn	S	Si	Cr	Fe
SS 302 A	0.074	0.024	8.430	0.710	0.001	0.578	18.399	-

Table 2.2: Alloy composition of SS 302 A fiber.
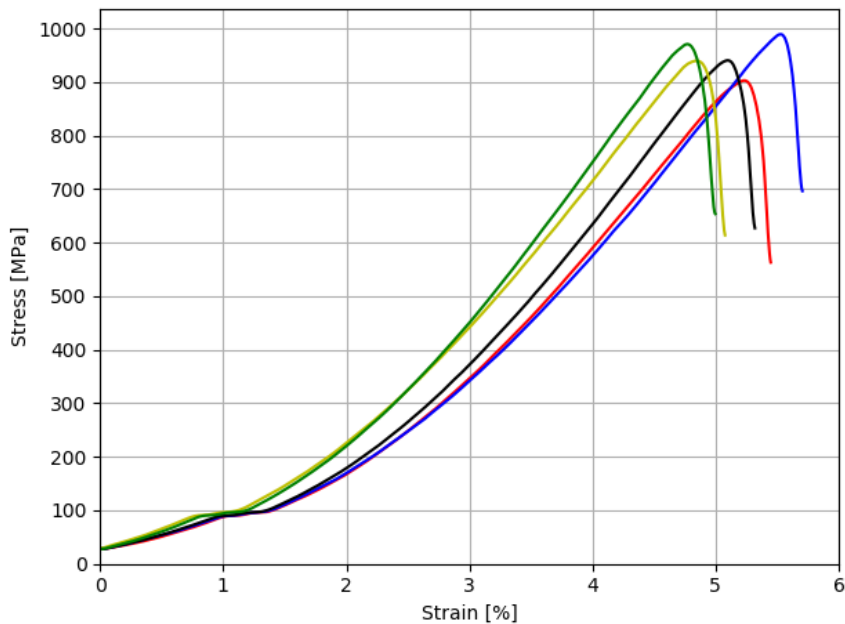
Figure 2.2: Fiber bundle tensile test of AISI 302A steel fiber.

2.2 Classification of Pressure Vessels

Pressure vessels are classified in four classes; Type I, II, III and IV. Were type I and II are made out of solid metal. Type III are made out of fiber reinforced polymer composite with a metallic inner liner. In this project, the pressure vessel is design as class IV. That means that the tank includes a inner layer, called liner, and fiber reinforced composite layer on the outside. The liner is usually of polymer like High-Density Polyethylene (HDPE), and the fiber is either carbon fiber/epoxy or a hybrid of carbon/glass fiber composition. The newest addition to the pressure vessel classification is the Type V pressure vessel. This is a linerless pressure vessel which is composed of only composite. Since this is such a new type of pressure vessel its is not yet an industrial standard, but certainly will be within few years.

2.3 Laminate Structure

When discussing the structural build of a composite, it is often referred to as a laminate. A laminate consists of layers, or plies, with one or more orientations with respect to the

orientation of fiber in the layer/ply. The term layer are commonly used in the mechanical and mathematical definition of laminates, while a ply often refers to parts of a layer that does not cover the whole laminate. In this thesis both layer and ply are used interchangeably because there are no differences in the amount of layers along the pressure vessel. The plies are symmetrically stacked with respect to the laminate midplane, i.e. there are identical amount of plies with the same ply orientation from midplane to the top of the laminate and equally from midplane to bottom, illustrated by the dashed line in Figure 2.3. The stacking sequence of the laminate is called the laminate lay-up. Arranging the plies in such a manner creates a balanced symmetric laminate, and is considered the optimal stacking sequence for axis symmetric components because the loading in any given plane does not lead to deformations in other planes. When referring to plies they are numbered ranging from bottom to top, with each of the plies having the same thickness. Therefore, a laminate described as $[\theta/90°]$ will have a θ ply at the bottom referred to as ply 1. For a laminate that contains different materials the plies will be denoted with regard to the material in that ply, e.g. $[90°_{2c}/\pm 15_{2C}/90°_{2s}]$ will have its two first plies in steel fiber and the rest in carbon fiber. The angle notation of the ply is in reference to the longitudinal direction of the pressure vessel. The plus/minus notation, ±15, means that it is referred to two plies with opposite angles.
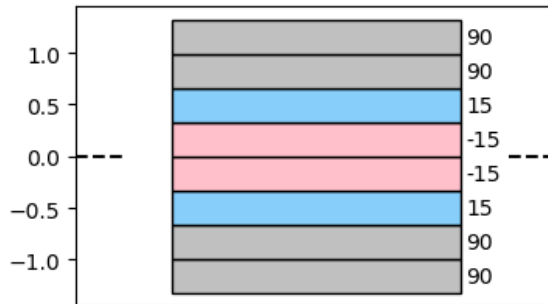
Figure 2.3: Stacking sequence of a $[90_2/\pm 15_2]_s$ laminate.

2.4 Hybridisation of Fiber

A hybrid composite made by different lamina materials are called a laminar hybrid. There are, to the authors knowledge, never been produced a pressure vessel using steel fiber or a hybrid of steel and carbon fiber. There is however done some research on hybridisation with steel and carbon fiber on flat laminate structures. Mosleh et al.[12] Due to

2.5 Determination of Laminate Properties

2.5.1 Pressure Vessels

The pressure vessel for this project is defined as thin-walled pressure vessel. To fulfill the thin-wall definition the thickness to internal radius ratio of the laminate part of the pressure vessel has to be greater than ten ($t/r_i > 10$). The common design of a pressure vessel contains two parts; the cylindrical part, and the spherical part. The cylindrical part will have principal stresses acting in both hoop and axial (helical) direction (equation 2.1 and 2.2). The spherical part, which is dome shaped end caps to the cylindrical section will have principal stresses acting only in axial direction. The stresses are illustrated in Figure 2.4. In general longitudinal direction refers to the line going from end to end of the pressure vessel.

$$\sigma_h = \frac{pr_i}{t} \tag{2.1}$$

$$\sigma_a = \frac{pr_i}{2t} \tag{2.2}$$

σ_a and σ_h are always in tension for a pressure vessel. r_i is the inner radius going from center to the inner part of the laminate, t is the total thickness of the laminate and p is the internal pressure acting on the laminate.
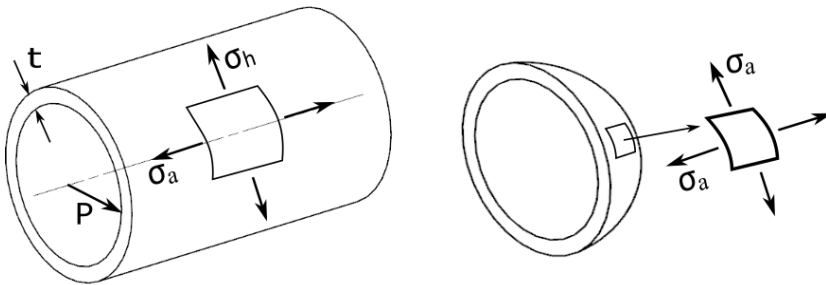
Figure 2.4: Principal stresses acting on cylindrical and spherical part of the pressure vessel.

For a Composite Overwrapped Pressure Vessel (COPV), the most critical failure mechanism is abrupt bursting from the internal pressure due to rupture failure. This means that the hoop stresses caused by the internal pressure in the vessel is the dominant failure mechanism unless the amount of hoop layers vs. helical layers are balanced. Other failure mechanisms that should be considered is impact load. This can be cause by dropping the vessel, tool drop, or a collision event.

2.5.2 Elastic Engineering Properties

To estimate the necessary thickness needed for the composite tank, the maximum allowed stresses caused by the internal pressure, also referred to as membrane loading, needs to be calculated. To simplify the procedure, the matrix is assumed to carry zero load. This procedure is called netting analysis [13]. It is a conservative approach that assumes only the fibers takes up load, and the matrix is only used to keep the placement of the fibers in the correct position. The thickness is needed for mainly two reasons, to find out how much strength that each layer is going to be able to carry and to find the amount of fiber material that is needed to produce the composite overwrap of the pressure vessel. The material thickness is divided into two thicknesses, t_θ for the helical fiber layers, and t_h for the hoop layers. The pressure vessel can be defined as a thin walled pressure vessel as long as the ratio of radius to thickness, r/t, is equal to or greater than 10. The stresses acting on the walls of the cylindrical part of the vessel, as mentioned earlier, is hoop and axial stresses. The stresses caused by the internal pressure produces a hoop to axial stress ratio of 2:1. This means that the hoop layers carry the most load and it is therefor a need to balance the amount of hoop layer for every helical layer.

There are nine independent elastic engineering constants required to define the mechanical response of a orthotropic composite. In most practical cases in accordance with Classical Laminate Theory (CLT) a state of plane stress is defined, and the out-of-plane stresses are disregarded. With a plane stress state it is meant that the stresses acting on the composite only appears as σ_1, σ_2 and τ_{12}. It can therefor be said that the mechanical properties of interest in a composite are E_1, E_2, G_{12}, ν_{12} and ν_{23}. The assumption of in-plane properties becomes; $E_2 = E_3$, $\nu_{12} = \nu_{13}$, $G_{12} = G_{13}$. The composite failure strength can be used to define the composite elastic engineering constants. The common way to find the failure strength is by defining the fiber alignment within a laminate layer as unidirectional.

In this thesis, to determine the elastic properties of the steel- and carbon fiber/epoxy laminate, calculations from CLT and micro-mechanical models in accordance with Vedvik [14] has been used. By using basic rules of mixture principles, the mechanical properties has been determined, and is presented below as Equation 2.3-2.7 [14]:

The longitudinal stiffness of the laminate, E_1, was found using the equation:

$$E_1 = V_f E_{1,f} + (1 - V_f) E_m \tag{2.3}$$

The notation $E_{1,f}$ is in reference to modulus of the fiber material, likewise is the E_m in reference to the modulus of the matrix/epoxy. V_f is the fiber volume fraction, i.e. the amount of area fiber vs. area matrix.

The transverse stiffness of the laminate, E_2, was found using the equation:

$$E_2 = \frac{E_{2f} E_m}{V_f E_m + (1 - V_f) E_{2f}} \tag{2.4}$$

The density of the laminate, ρ, was found using the equation:

$$\rho = V_f \rho_f + (1 - V_f) \rho_m \tag{2.5}$$

The Poisson's ratio in 12 direction of the laminate, ν_{12}, was found using the equation:

$$\nu_{12} = V_f \nu_{12f} + (1 - V_f)\nu_m \tag{2.6}$$

The shear modulus of the laminate, G_{12}, was found using the equation:

$$G_{12} = \frac{G_{12f}G_m}{V_f G_m + V_m G_{12f}} \tag{2.7}$$

The shear modulus in 13 direction is defined as the same as the matrix shear modulus.

A symmetric laminate means that it is both geometric and material symmetry with respect to the mid-plane. To determine geometrical symmetry in the laminate there needs to be identical ply orientation above and below the mid-plane. To have material symmetry it is required that the whole laminate contains of the same material, or that the different material plies are symmetric with regards to the mid-plane. If both these requirements of symmetry are fulfilled, the B matrix can be considered zero ($B = 0$).

Chapter 3

Production method

3.1 Design of Pressure Vessel

The pressure vessel are composed of two main regions, the cylindrical part, and the end-caps (domes) on each side of the cylindrical part. Since the pressure vessel is designed to be produced through filament winding, some limitations and problems comes with the production procedure. The main limitation is the angle that the helical layers can be applied by the filament winding machine. When winding with a narrow angle, in the range of $0° - 10°$, the fibers that is applied at the end-caps tends to slip. Fiber slipping is usually due to the lack of friction from the rapid change in geometry at the domes. This will cause gaps in the composite and therefor will not be properly sealed or take up stresses as intended. From earlier experience with the filament winding machine, it was decided to design the tank with helical layers of $\pm 15°$.

When determining the stacking sequence it is important to consider in what order the hoop and helical layers are placed. It is generally considered important to place the hoop layers outside the helical layers to incorporate the helical fibers better. When there are no hoop layers within the helical layers, the helical fibers tends to pull away from the laminate in a localized mode of failure. This is called fiber pull out. Therefore, it is advantageous to vary with helical and hoop layers, placing hoop layers at top and bottom of the laminate.

From the Hipactor project of Saeter et al.[4] there were produced pressure vessels with CFRP composite overwrap with stacking sequence $[90_2/\pm 15_2/90_2]$. It was decided to produce the pressure vessels in this thesis with the same stacking sequence to reduce the amount of pressure vessels needed to produce.

3.2 Filament Winding Production

The core principal of filament winding is to draw tensioned fiber through resin/epoxy and apply it on a mandrel. Table 3.1 shows the material properties of the carbon fiber, steel fiber, and epoxy matrix used in the filament winding production in this thesis.

Mechanical Properties	Material		
	SS 302 A	Toray T700S	EPIKOTE MGS RIMR 135
Elastic modulus [GPa]	200	230	3.2
Tensile strength, σ_{UTS} [MPa]	950	4600	65
Strain-to-failure [%]	3-5	1.8	12
Poisson's ratio	0.30	0.30	0.35
Density [g/cm^3]	8	8	1.2

Table 3.1: Mechanical properties of stainless steel with $d = 8\mu m$, carbon fiber with $d = 8\mu m$, and epoxy resin. [2]

Two different composite products were produced by filament winding; ring specimen for split disk testing, and pressure vessel for burst and impact testing.

In this section the production procedure used to produce all the composite products for the thesis is discussed in detail. This is both for the ability to assess the quality of the production, and to have the ability to reproduce the production. It is worth noting that this becomes specific to the filament winding machine used at NTNU, and that every machine will have its own specifications and offsets that differs from others. The filament winding machine used in this thesis was carried out on a four-axis Microsam automated machine (Figure 3.1). With it is a tension cabinet that the fiber materials are connected to from their spools and applies constant tension on the fiber through load cells during the filament winding process. From the tension cabinet, the fiber goes through a resin impregnation bath that can be seen in Figure 3.3. Here the big wheel, or drum, draws resin from the tray that is placed under the drum and coats the fiber that lays on top of the drum with resin. To adjust the amount of resin that coats the fiber the doctor blade that lies close to drum can be hand-adjusted. There are no motors involved with the impregnation system, the fiber drives the drum around and the speed is controlled by the winding speed. The sufficient resin level of the impregnation system is based on the users experience with the production method, as it is needed to assess if the fiber gets impregnated with the right amount of resin by visual means during the winding process. After the fiber has passed the resin impregnation bath and coated with resin it goes through the "feedeye" of the filament machine (Figure 3.2). The feedeye is keeping the fiber tow spread out to its bandwidth and it is from here the fiber is placed onto the mandrel and end-domes. During the winding process the placement of the fiber might be disturbed by fiber slipping at the end-domes or fiber breakage. What is usually done, but not always necessary, is applying pressure to the fiber as it is placed on the end-domes. This keeps the tension on the fiber when the winding machine changes direction of the eye. When fiber breakage occurs the tension cabinet register that there is an error and stops maintaining tension on the fiber. Then the winding machine needs to be stopped and the broken fiber needs to be

spliced together before the winding process can be continued. Splicing leaves a knot that is visibly thicker than "healthy" fiber, but when fiber is wounded over it, there is hardly any dent. It is worth noting that this will most likely leave a higher void content and should be considered as a weakness in the composite. From experience the winding programs that are made in Winding Expert do not handle multiple tasks, therefor the programs are made individually, i.e. into separate hoop and helical programs with regards to correct bandwidth. The winding programs are CNC codes that orientates the filament machine with positional information of radius and length of the mandrel, angle of fiber, and shape of end-domes. When the winding process is completed and access resin is scraped off, the mandrel is set to rotate while the resin cures in room temperature for 24 hours. After the 24 hours of curing is completed the composite is heat cured at 80°C for 16 hours, which will further increase cross-linking in the polymer. The Epoxy resin used in this thesis is

Figure 3.1: MicroSam automated filament winding machine during production of composite tubes.

3.2.1 Pressure Vessel

The pressure vessel programs are divided into two sections; Hoop winding and helical winding. The hoop winding is defined by the mandrel part of the pressure vessel, and is relatively straight forward. It take two arguments; length and radius. As for the dimension of the mandrel used it is assumed that the radius is constant in the setup, but in reality the mandrel is more eye-shaped. This eye-shape will cause some offset in the placement of the fiber, but there has not been observed lack of quality because of it. The mandrel length used in the production was 590mm of effective length. On each side of the mandrel there is an additional 25mm extension of turned "lip" where the end-domes overlap with mandrel.
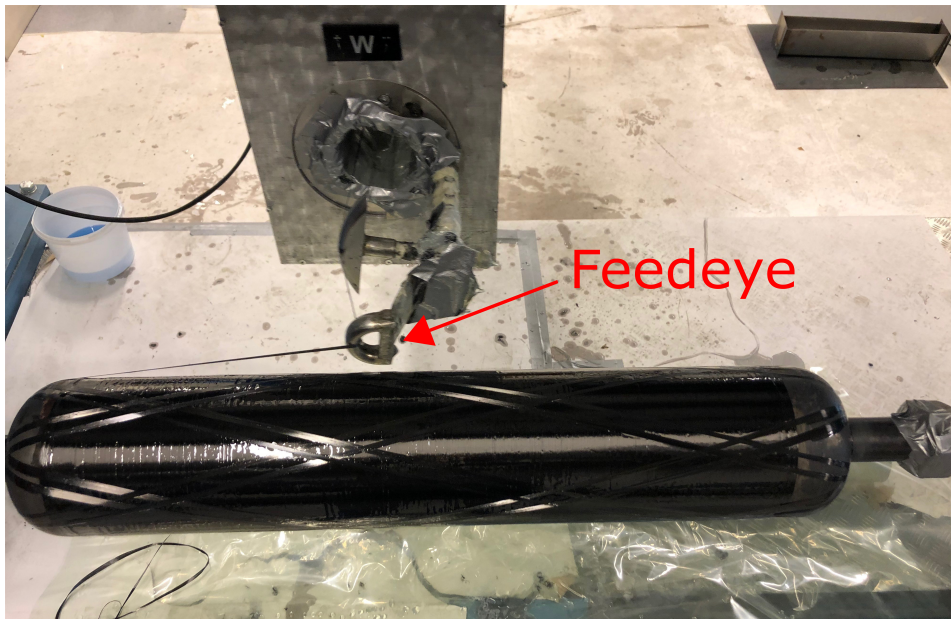
Figure 3.2: Helical winding during pressure vessel production.

The helical winding needs more inputs to wind with accuracy. Defining the end-dome section of the pressure vessel is more complicated to get accurate, and requires some trail and error to get right. Each side the end-domes must be defined such that the filament winding machine is able to orientate the shape of the end-domes such that the fiber can be applied with correct angle, to not crash the feedeye in the end-domes, and to withstand fiber slippage. In Table 3.2 the dimensions of the mandrel and end-domes are defined.

For the hoop layers, the program only takes the arguments for the mandrel part. For the helical layers, the program takes the arguments for the end-domes.

After the post curing is completed the pressure vessels were injected with thin polyurethane liner to make sure to have pressure tightness. The polyurethane used was a 1:1 mixture of HPE 40 A Polyol and HPE 40-85 iso [15] which cured at room temperature for 24 hours.

3.2.2 Ring Specimen

The productions of the composite used to make ring specimens started with winding composite tubes on a HDPE mandrel with outer diameter of 140mm. The winding expert setup used in the procedure is a simple hoop program. The hoop program takes only inputs for the mandrel, i.e. diameter and length of the mandrel. Three different material configuration was used to make three different composite tubes; Steel Fiber Reinforced Polymer (SFRP), Carbon Fiber Reinforced Polymer (CFRP), and a hybrid of SFRP and
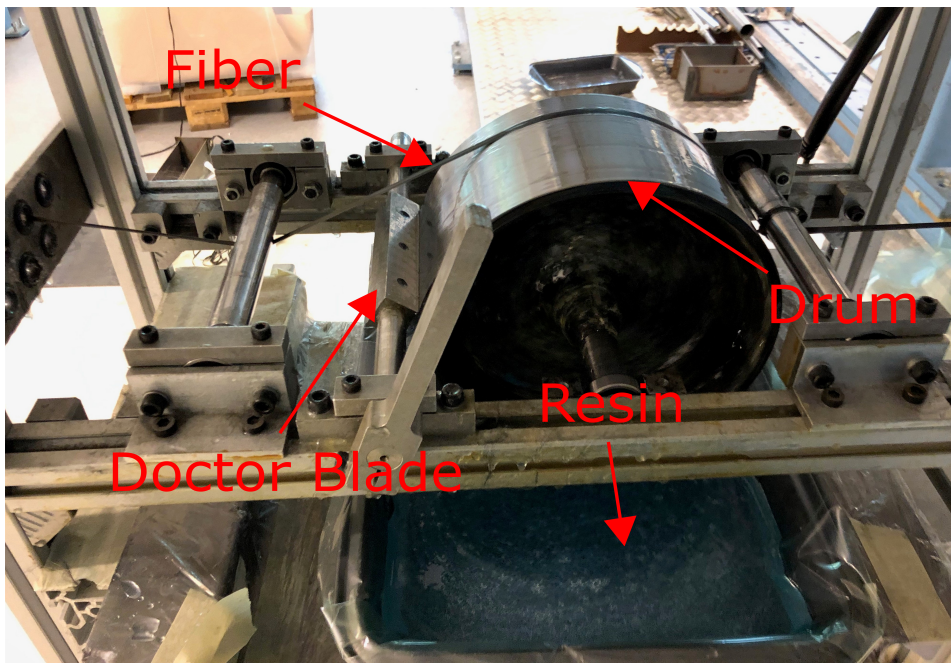
Figure 3.3: Impregnating resin bath.

CFRP (hybrid). As the bandwidth for the steel and carbon fiber is different they needed to use two different programs, but the winding angle is considered to be the same for the hoop placement. All the composite configuration were wound with four hoop layers.

After the full curing process was completed, the composite tubes were cut into ring specimens in preparation for split disk testing according to ASTM D2290-19 [3]. The ring specimens were cut using a water cooled band saw and the edges polished to remove cut marks. The width of the rings was limited to the width of the split disks (section 4.2) and the load capacity of the test machine (100kN). To make sure the load capacity of the tensile machine did not get exceeded for the CFRP ring specimens some rudimentary strength calculations was done. To remove the mandrel from the ring specimens they were put in a freezer for a couple of hours. When cold enough the mandrel will shrink more than the composite, and it is easy to separate them. The thickness and width of the ring specimens were measured extensively with a micrometer, the dimensions can be seen in Table 3.3. Cross-section samples for quality control of the specimens were also provided. This was used mainly for the microscopic analysis and burn-off test to determine the fiber volume fraction (section 4.4 and section 4.5).
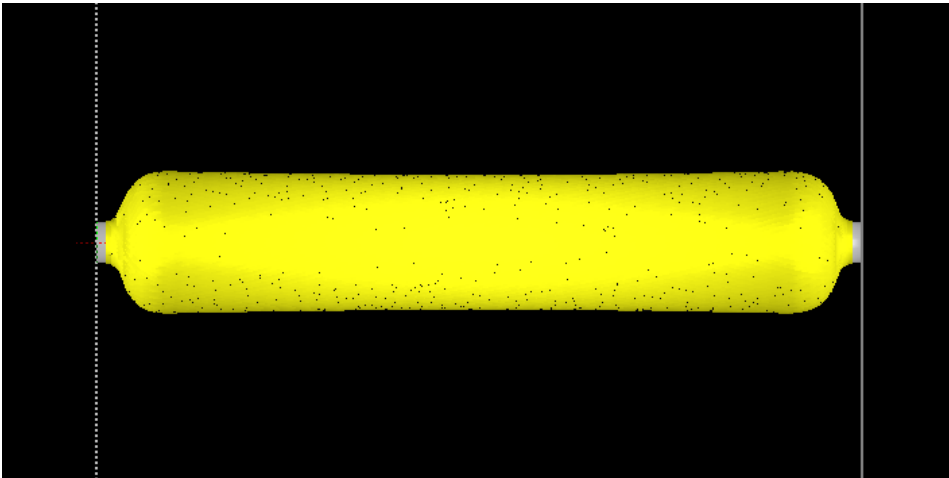
Figure 3.4: Simulation of helical fiber pattern in Winding expert.

	Section	
Winding parameters	Hoop	Helical
Winding angle	89°	±15°
Fiber speed [m/min]	20	20
Cycles	1	89
Coverage [%]	100	104.8
Pattern	-	-5/2
Bandwidth:		
SFRP [mm]	2	-
CFRP [mm]	5	5
Pre-tension:		
SFRP [N]	20	-
CFRP [N]	40	40

Table 3.2: Winding expert parameters
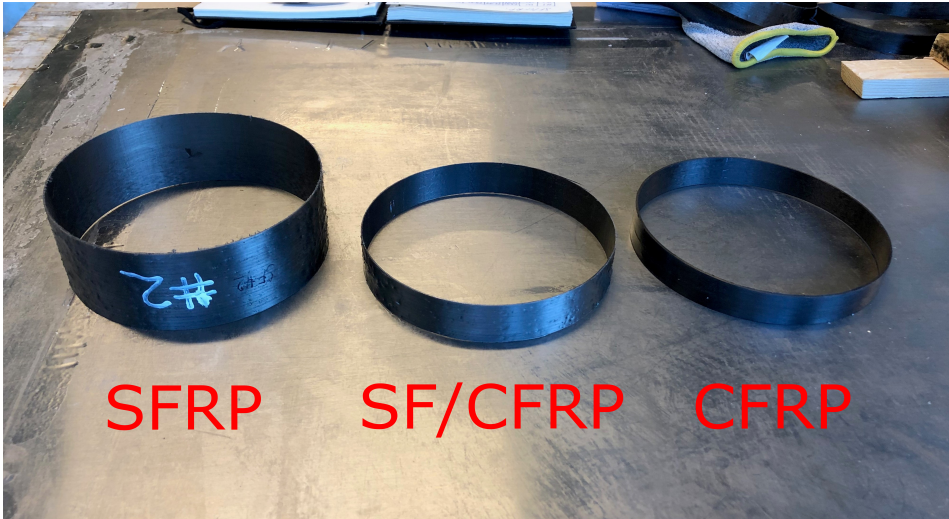
Figure 3.5: Prepared ring specimens for split disk testing

Sample	Measurements		
	width, W [mm]	D [mm]	thickness, t [mm]
SFRP [90_{4S}]:			
1	47.865 ± 0.340	140	1.105 ± 0.079
2	48.980 ± 0.096	140	1.145 ± 0.096
3	48.940 ± 0.752	140	1.060 ± 0.125
4	45.243 ± 0.346	140	1.138 ± 0.056
CFRP [90_{4C}]:			
1	19.188 ± 1.154	140	1.510 ± 0.062
2	19.528 ± 0.158	140	1.485 ± 0.051
3	18.270 ± 0.898	140	1.533 ± 0.036
4	20.225 ± 0.321	140	1.400 ± 0.062
SF/CFRP [$90_{2C}/90_{2S}$]:			
1	23.738 ± 0.511	140	0.950 ± 0.045
2	23.140 ± 0.882	140	0.863 ± 0.049
3	24.313 ± 1.248	140	0.925 ± 0.055
4	26.975 ± 0.487	140	0.963 ± 0.118

Table 3.3: Dimensions of the samples for split-disk testing

Chapter 4

Test Setup and Experimental Method

4.1 Fiber Bundle Tensile Test

The mechanical properties, Ultimate Tensile Stress (UTS) and strain-to-failure, for the AISI SS 302A used in this thesis is based off of fiber bundle tensile testing. The test fixture includes two clamps that allows for the steel fiber to wrap around the clamps to reduce the stress concentration, that are common in flat clamp fixtures, the test were conducted with a MTS 5kN tensile machine (Figure 4.1).

4.2 Split-Disk Testing

To investigate the tensile strength of the steel fiber, both as a solely reinforcement fiber and in a hybrid configuration with carbon fiber, a split-disk test method was used. In accordance with standard ASTM D2290 [3] a split-disk test is preformed to obtain hoop tensile strength of the filament wound composite. Split-disk test, when properly interpreted, provides relatively accurate information about the tensile strength of composite pipes when employed under similar conditions. It is widely used as it is an unambiguous procedure compared to the hydro-burst method, which requires extensive preparation. It is worth noting that the split-disk method has a drawback, as it induces lower failure stress and strain. This is due to stress concentration in the ring specimen located at the split of the two half-disks. It is also necessary for the failure to occur at the split region between the two half disks to obtain accurate results. Split-disk test considers the strength characteristics of fiber reinforced composite with continuous aligned fiber that is loaded in the longitudinal fiber direction. These conditions makes it possible to obtain the ultimate tensile strength
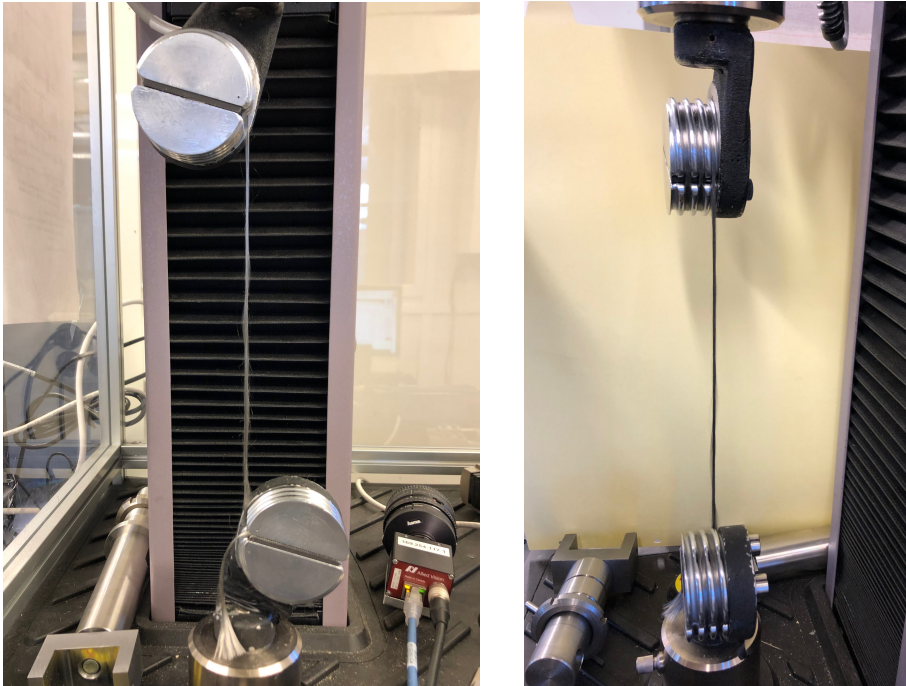
Figure 4.1: Test setup of the fiber bundle tests.
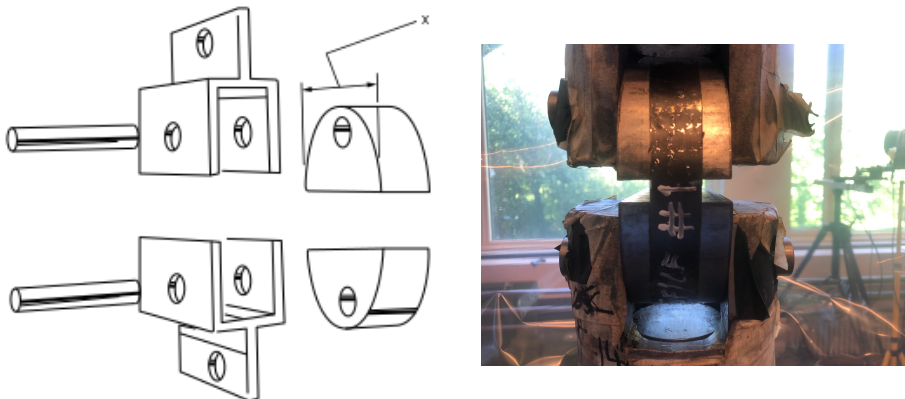
Figure 4.2: split-disk test. On the left is a schematic of the test rig [3]. On the right is a hybrid ring specimen attached to the test rig.
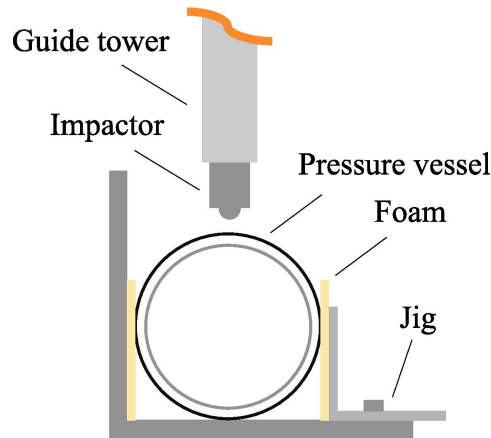
Figure 4.3: Schematic of impact test setup. [4]

of the composite on the stress-strain curve that corresponds with fiber failure, and can be defined as the point of composite failure.

4.3 Impact and Burst Testing

Two experimental tests were conducted on the pressure vessels; impact testing and burst testing. One pressure vessel was damaged through impact testing before burst tested, and one vessel was only burst tested.

The impact test were performed without any internal pressure in the vessel during the test. The impact test was carried out using a drop tower assembly shown in Figure **??**. The impactor used was steel hemispherical shaped with =20mm. The pressure vessel were clamped between two vertical profiles shown in Figure 4.3. To protect the pressure vessel while clamped a layer of foam were fitted between the vertical profiles. The impactor was dropped on the middle of the cylindrical section of the pressure vessel from a height of 1.43m (60J).

In preparation for the burst testing the pressure vessel were fitted with strain gauges to monitorize the pressure vessels during pressurization. The strain gauges used were of the type FLA-5-11 by Tokyo Sokki Kenkyujo, which has a gauge length of 5mm. Six strain gauges were mounted on the surface of the pressure vessels, both in hoop and axial direction spaced out in three groups located at the center of the cylindrical section of the pressure vessels.

4.4 Image Analysis

Microscopy analysis allows for determination of void and fiber volume fraction. The sample used to conduct the microscopy analysis was prepared by cutting cross-section of the SFRP and molding it in epoxy. Then the mold, or puck, was grinded down with progressively finer coarseness until the sample yielded a cross-section of the fiber/epoxy composite. The fiber volume fraction of the SFRP was calculated through image analysis. The finished sample can be seen in Figure 4.4. Looking at the cross-section sample through
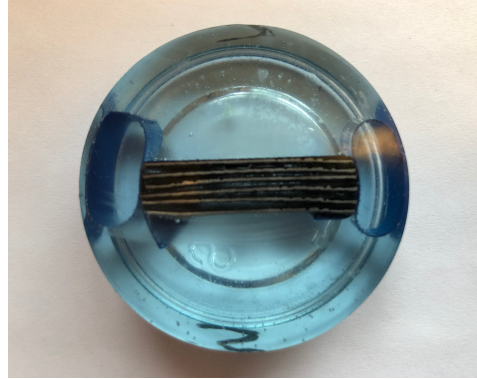
Figure 4.4: Cross-section sample used for microscopy analysis

microscope makes it possible to calculate the fiber volume fraction, Figure 5.1 shows the microstructure of steel fiber reinforced composite. The fiber volume fraction was found by running the image through a script [16] that analyses the different gray-scale values of the image, and defines the profile of the fibers.

4.5 Burn-off Test

To be able to determine and confirm the fiber volume fraction of the composite, a burn-off test was conducted. The burn-off method works by heating the composite to a temperature where the polymer matrix decomposes in to a gas, while the fiber does not. SFRP composite samples was placed in ceramic cups and weighted before placed in an oven at $550°C$ for 3 hours. The post heated sample is weighted, and by using 4.1 the fiber volume fraction was determined. The assumption is that a small specimen of the large composite will represent the fiber volume fraction for the whole composite.

$$V_f = \frac{m_f \rho_m}{m_f \rho_m + m_m \rho_f} = \frac{W_f / \rho_f}{W_c / \rho_c} \tag{4.1}$$

This approach does contain several sources of error. For the burn-off test to be accurate, the void count needs to be taken into consideration. Having a relatively moderate amount

of voids in the composite will have a high influence on the result if not accounted for. Also when working with carbon fiber the size will decompose at elevated temperatures. As for the steel fiber, which has no size, this will not be a problem. There will be some oxidization on the steel fiber, but this has been deemed too insignificant amount.

4.6 Micro-mechanical Model

To compare the calculated elastic engineering properties presented earlier, a micro-mechanical model was simulated through Finite Element Method (FEM). This approach uses a Representative Volume Element (RVE), or unit cell, to represent the volume of the material that exhibits statistically homogeneous material properties (Figure 4.5). The RVE is the smallest volume that can be used to represent the whole layer in a composite with a repeating structure. By using a unit cell to represent the whole layer it makes the same assumptions as CLT about homogeneous with in layers. The unit cell represents a hexagonal configuration of the fiber/matrix. The FEA model used is representing a hexagonal configuration of the fiber/matrix in a unidirectional composite. The hexagonal pattern can be seen in Figure 5.1, and is proven to be an realistic and accurate approach than square pattern for finding elastic properties of fiber reinforced composites.

4.7 Non Destructive Testing

One of the hypothesised benefits of using steel fiber to reinforce composites was that it allows for Non Destructive Testing (NDT). This can be used to check if there are any fiber breakage in the composite. Ultrasonic testing is commonly used. The test run with a ultrasonic sensor did not yield any definite results that fiber breakage or damage is easily detected when working with steel fiber. Therefore it was decided to not further investigate this, as it is both time consuming and not a main priority for the thesis. The approach and results are described in Appendix 7.
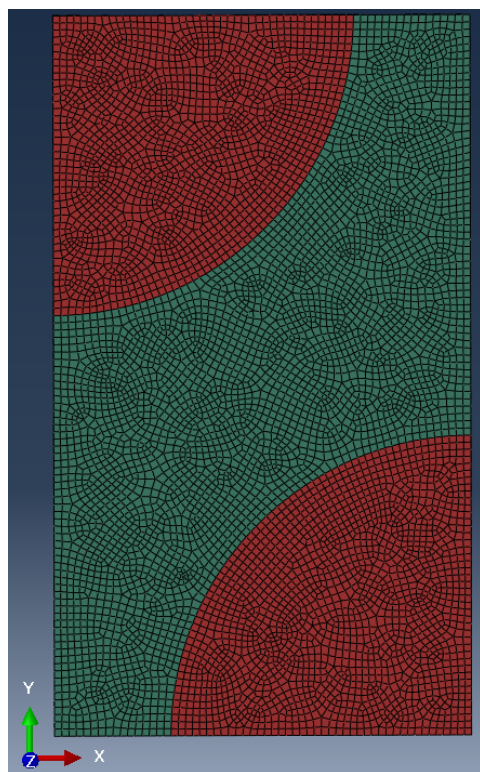
Figure 4.5: Mesh of unitcell.

Chapter 5

Results

In this chapter all the results from the theoretical calculations, analytical analysis and experimental tests conducted in this thesis will be presented.

5.1 Investigation of Product Quality

The fiber volume fraction, V_f, was found by microscopic image analysis and burn-off test. The results from the image analysis is only done for the hybrid sample of SF/CFRP, but it is assumed that the results are transferable to the other samples also. Table 5.1 shows the volume fraction results as separate composites for the image analysis, and only SFRP for the burn-off.

Sample	V_f^a [%]	V_f^b [%]
SFRP	54.4±3.28	45.7±1.12
CFRP		54.5±2.03

Table 5.1: Results from: [a] Image analysis. [b] Burn-off test.

Figure 5.1 shows two samples from the microscopy investigation that are taken inside SFRP layers. They show that the steel fiber are tightly compacted and well impregnated with epoxy resin. The voids in the composite was easier to identify for the CFRP layers, but in general the void count was low for the cross-section samples investigated (Figure 5.2). The fibers can be seen having a hexagonal configuration as assumed for the micro-mechanical model in Section 4.6. When running image analysis with images from inside the SFRP layers the local volume fraction for the fiber is as high as 75%. In Appendix 7
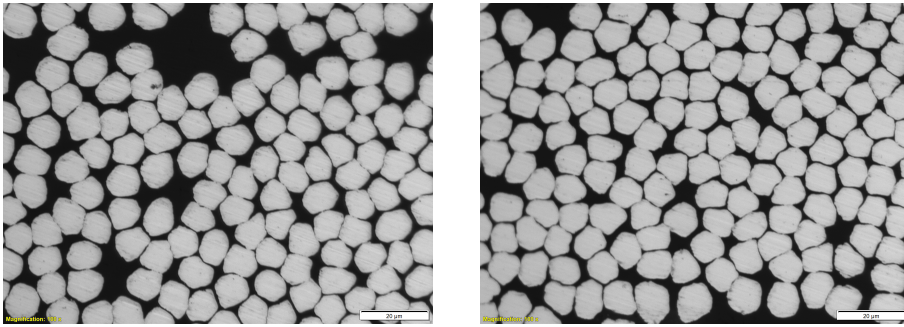
Figure 5.1: Image of SFRP with magnification of 100x.

more images can be seen that have been used to determine the volume fraction and also measuring the layer thickness of both CFRP and SFRP composites.

As mentioned earlier, the burn-off test is providing a lower V_f as it takes the whole composite into consideration. This means that the layer of epoxy that is on the outer layer of the fiber is part of the V_f. By including the outer epoxy layer, the V_f becomes lower while only contributing to the elastic property E_2. Epoxy tends to gather in the outer layers in the filament winding process, as excess resin gets forced to the outside as the fibers are placed on top of each other. Usually some of this excess resin are scarped of at the end of the winding production, but there can only be removed so much by hand. As Table 5.1 shows, the volume fraction values obtained between image analysis and burn-off test differ with as much as 10 percentage points. Therefore, as a conservative approach, all the calculations conducted on the elastic properties of the composites in this thesis uses the values from the burn-off test. This includes also the micro-mechanical model analysis.

The microscopy images showed no cracks between layers of both CFRP and SFRP. The transition between CFRP and SFRP looks to be strongly bonded with little excess resin between them. The layers of both CFRP and SFRP could, in some instances, be difficult to identify due to both overlapping and compact fiber configuration between layers.

5.2   Calculation of Composite Properties

The elastic properties were calculated by using the formulas as shown in Chapter 2. The result from calculations and Finite Element Analysis (FEA) is shown in Table 5.2.
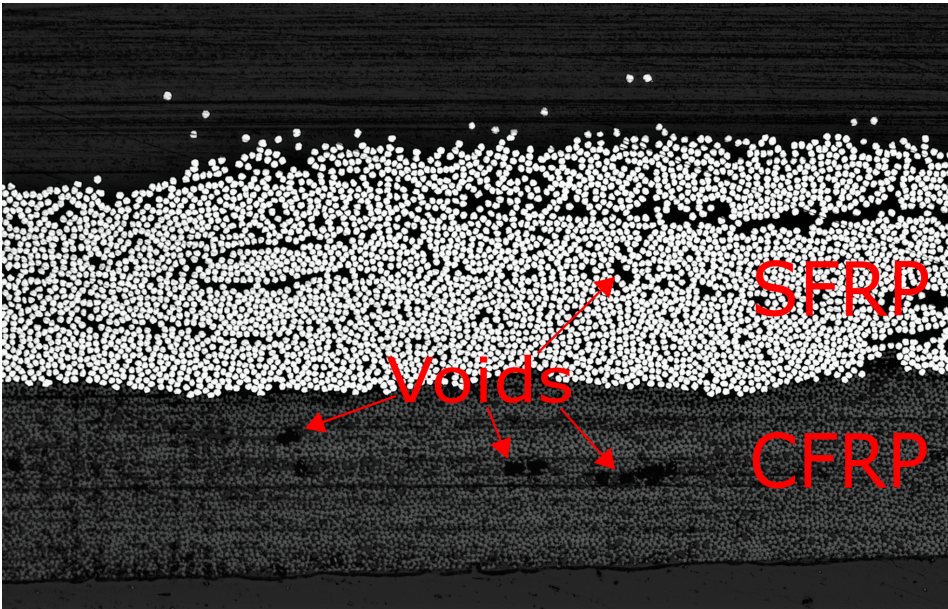
Figure 5.2: Microscopy image of hybrid composite cross-section.

Engineering properties	SFRP		CFRP		Hybrid	
	Material					
	calculated	FEA	calculated	FEA	calculated	FEA
E_1 [GPa]	93.14	95.98	120.9	126.4	110.54	106.8
E_2 [GPa]	5.82	4.99	6.6	5.89	6.40	5.45
δ [g/cm^3]	4.31		1.51		2.92	
G_{12} [GPa]	2.12		2.4		2.13	
G_{23} [GPa]	1.19		1.19		1.19	
ν_{12} [-]	0.327	0.323	0.324	0.321	0.325	0.323

Table 5.2: Material properties for the composites

5.3 Split-disk Test

The split-disk test was done with a Instron 100kN tensile machine. All the samples were subjected to displacement controlled speed of 1mm/min and results can be seen in Table 5.3. In the preparation to the test setup the ring specimens were subjected to a pre-load of around 15N before the test started. The SFRP ring specimens all broke due to fiber failure

Figure 5.3: SFRP ring specimen after split-disk test.

in a rapid, symmetrical, fashion. All four samples broke on one side with little to no debonding between the layers. The samples had multiple through-the-thickness interfiber failure that ran mostly the whole way around the samples (Figure 5.3).

The hybrid ring specimens experienced fiber failure in the steel fiber part, dropped about 1/4 in stresses, before starting to take up stresses in the carbon fiber layers again (Figure 5.4). As the test continued to run, the carbon fiber layers had sporadically fiber failures until ultimate failure occurred. Similar with the SFRP ring specimens, the steel fiber layers of the hybrid rings broke in a brittle manner all at one side with no debonding on the opposite side between the steel and carbon fiber transition.

The CFRP ring specimens broke by fiber failure (Figure 5.5) and showed interlaminar

Figure 5.4: Broken hybrid samples. To the left: hybrid sample with first-ply-failure in SFRP layers. To the right: hybrid samples that experienced ultimate fiber failure

Figure 5.5: Broken CFRP ring specimen

failure. The failure occurred as rapid rapture, and the fibers broke at different points on the ring. There were no progressive ply failure as was observed with the CFRP part of the hybrid ring samples. Some debonding between the layers could be observed.

Figure 5.6 shows a stress-strain curve from the split-disk tests for the three composite configuration. The test ran to complete failure and all the samples can be seen to exhibit a linear elastic stress-strain behaviour until either ultimate tensile strength (SFRP and CFRP) or first-ply-failure (hybrid). The hybrid samples experienced the lowest elongation until failure (0.9%) when the SFRP layers of the composite broke, after that they started picking up load in the CFRP layers of the composite. Throughout the continuation of the test the CFRP layers of the hybrid configuration experienced local fiber failures that until ultimate fracture. The hybrid ring sample finally broke at around 1.9% strain. The CFRP ring samples had the highest stress of all the composite configurations and broke at a strain-to-failure of 1.8%. The SFRP ring samples took up the least stress and broke at Ĩ.1% strain. There can not be identified any distinct yield region in any of the ring samples in neither composite configuration. All samples experienced an ultimate failure in a brittle fashion, with no necking observed.

Figure 5.3 shows the mechanical properties derived from the split-disk test.
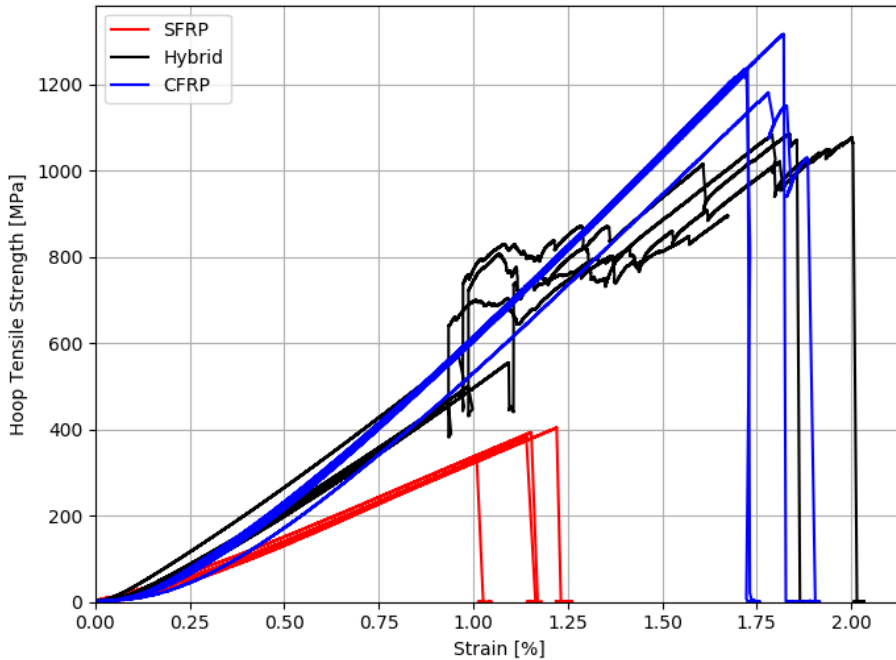
Figure 5.6: Results from the split-disk test

5.4 Impact and Burst Testing

The impact test left an imprint from the impactor and a matrix crack propagated in longitudinal direction of the pressure vessel, shown in the top image of Figure 5.8. There could be identified some fiber fracture originated from the matrix crack, but in a small degree. Figure 5.8 also shows the result of impact test from Saeter et al. [4] with the same impact energy on CFRP hoop overwrap. Here it is observed fiber fracture too much higher degree that propagated from both sides of the impact imprint.

The burst test on the pressure vessels did not yield any failure in the composite. Insufficient sealing inside the pressure vessel started a leak in both pressure vessel at around 20 and 30 bar. Figure 5.9 shows the results from the strain gauge measurements vs. internal pressure.
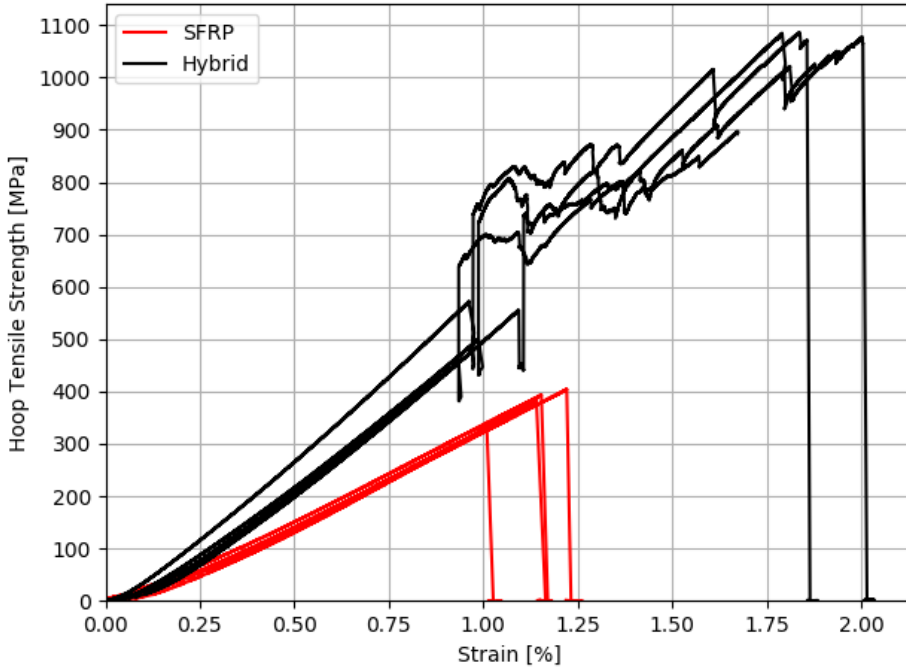
Figure 5.7: Results from the SFRP and hybrid split-disk test.

Mechanical properties	Test specimen			
	SFRP	$Hybrid^a$	$Hybrid^b$	CFRP
UTS [MPa]	377.9±32.8	521.0±53.3	1035.9±74.3	1240.7±56.8
Strain-to-failure [%]	1.16±0.09	1.01±0.07	1.89±0.16	1.83±0.08
E_1 [GPa]	70.7±2.7	105.8±8.3		110.6±1.1

Table 5.3: Mechanical properties derived from split-disk results.
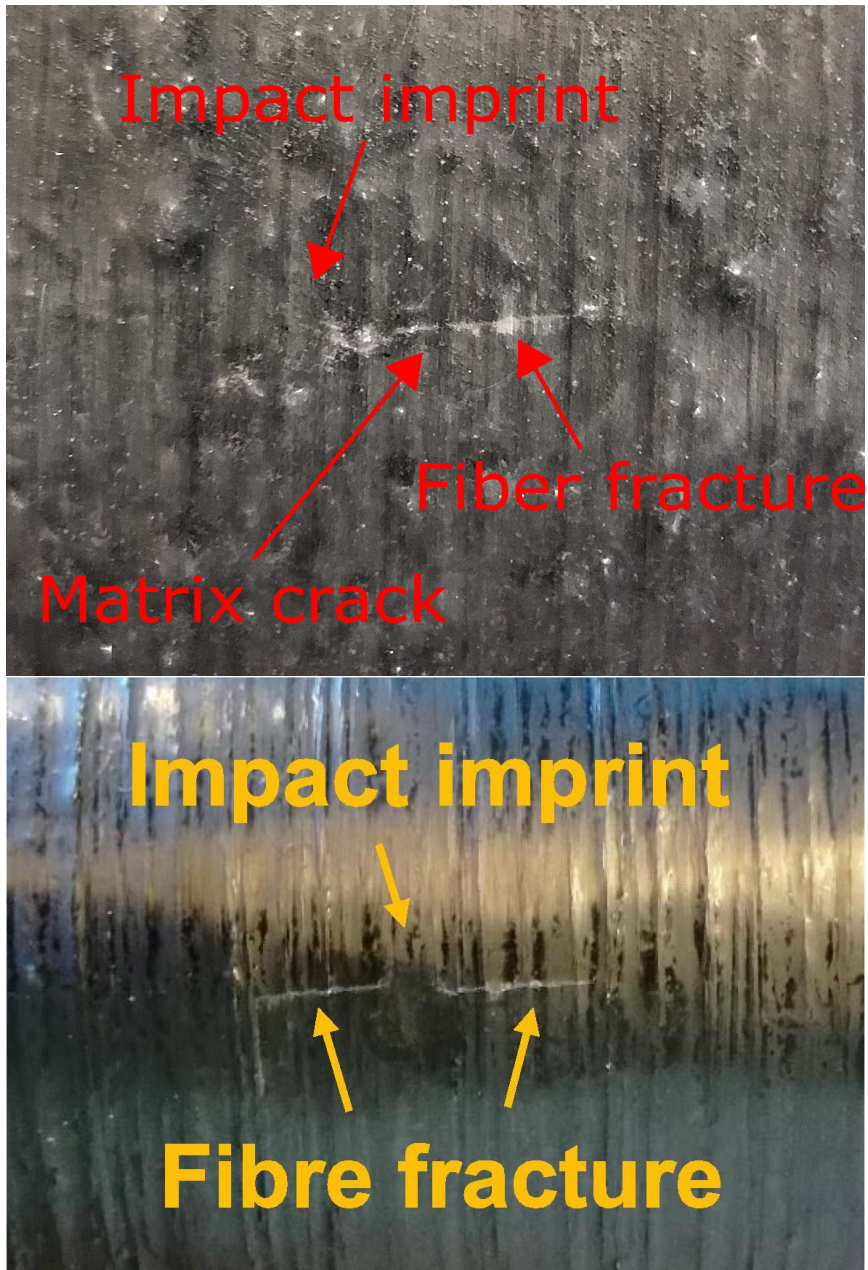
Figure 5.8: Figure top: Impact damage on SFRP overwrap. Figure bottom: Impact damage on CFRP overwrap.
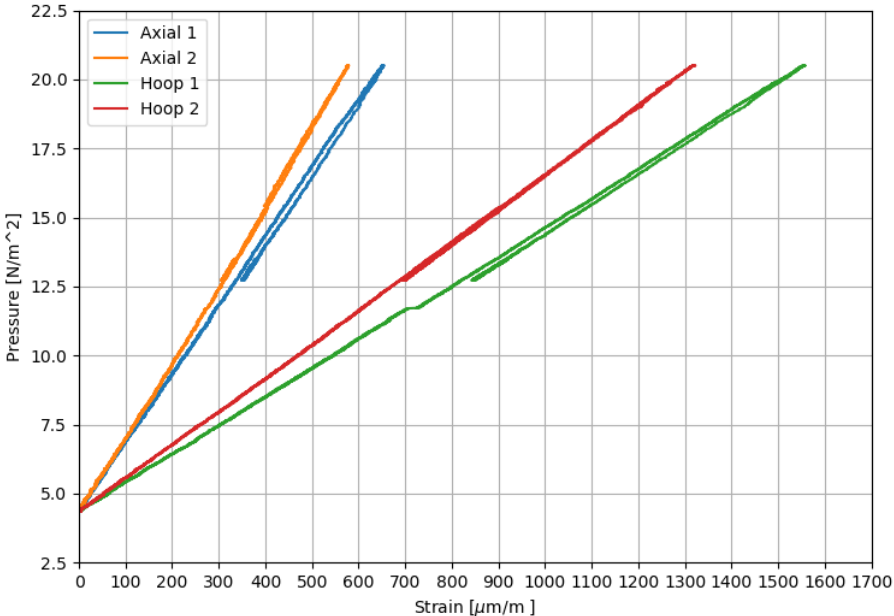
Figure 5.9: Burst testing.

Chapter 6

Discussion

This study has investigated the possibility of introducing steel fiber in pressure vessels for storing high pressure gases. As mentioned earlier, the main disadvantage of using carbon fiber when producing advanced composites is the cost and low strain-to-failure. The strongest contender of the metallic fibers considered to replace carbon fiber, is shown to be steel fiber. This is because it is the only metallic fiber that has satisfied the requirements such as strain-to-failure, stiffness, strength, and availability. The use of steel fiber introduces a number of problems when trying to cover the benefits of carbon fiber such as the low density and high tensile strength being the largest. Since the strength-to-weight ratio of carbon is far superior than any other fiber material available in the market, the applications the steel fiber composites can replace carbon fiber needs to be installations where weight is not an issue. This would be in the domain of marine tank- and bulk transportation. Here, storage vessels made out of 302A stainless steel would be a viable option, as the cost of the application can be driven down. Since corrosion is problem when steel is introduced to a application, the steel alloy needs to have great corrosion resistance. This restricts the option to use stronger steel alloys e.g. with higher carbon content to increase the tensile strength.

The main focus of this study has been to look at the effect of hybridization between steel and carbon fiber. This was achieved by producing the ring samples as described and can be considered a successful production. The same goes for the pressure vessels produced, but during burst test both the pressure vessels produced proved to not be sealed tight.

6.1 Production of Composite

With the production procedure of filament winding comes several uncertainties in terms of the quality of the end product. The quality of the production depends in many cases off the experience of the user. From making sure that the fiber goes untwisted from the fiber

spool to when its applied to the mandrel to coating the fiber with sufficient amount of resin there are aspects to take into consideration when accessing where faults and weaknesses may occur in the final composite product.

Cohen[17] lists the main driving parameters for filament wound composite pressure vessel as; winding tension, stacking sequence, winding time, and winding-tension gradient. By improving these parameters the main mechanism influenced is the fiber volume fraction. In general one can say that the higher the fiber volume fraction is, the more the composite strength increase. Cohen reported that the winding tension and winding time affects the fiber volume fraction the most. Winding with a high fiber tension yields a higher volume fraction. Similarly, low winding time produces higher volume fraction than longer winding time. The reason these two parameters (high tension and lower winding time) produces a higher volume fraction is to do with the fiber motion through the resin. By having a higher fiber tension when winding leads to larger fiber compaction which is also increased by low winding time due to the resin having a lower viscosity. The winding time of the tubes used for the split-disk test did not take long since there were only winding in hoop layers. For the production of the pressure vessel, the winding time was much longer. The first vessel took almost 4 hours to finish, while the second vessel took a little over 3 hours. The pot life of the epoxy used was reported to be 4 hours, which is notable during production as the resin increases its viscosity the closer to pot life it gets. The main reason for the first pressure vessel took longer to produce is because of fiber failure during the helical winding. Splicing the broken fiber and cleaning spilled resin is somewhat time consuming and lead to a temporarily stop in the production. The cause of the fiber breakage was loose carbon fiber piling up on one of the rollers in the impregnation resin system. As with the fiber tension different tensions were used depending on the fiber material. For the carbon fiber winding the fiber tension used was 40N, and for the steel fiber winding the tension was 20N. The reason for the lower tension on the steel fiber compared to the carbon fiber was that the steel fiber tended to break frequently when using 40 and 30N. Since the winding time of the production of the composite tubes did not differ much for the different configurations, the main parameter affecting the composites used in this thesis would be the fiber tension. This can be the reason as to why the CFRP composites has shown to have a higher volume fraction than what was found for the SFRP composites.

The lower volume fraction could be caused by the fiber not being saturated enough by the resin impregnation system. As the system is dependent on a user experience basis on both the controlling of doctor blade and visual inspection of the fiber after impregnation, it leaves uncertainties that are difficult to quality check. Ways to improve the resin impregnation of the fiber could be to operate with a lower winding speed. By further saturating the fibers with resin could help lowering the void count of the composite. But as discussed the winding time and the effect of increasing viscosity of the resin, this would counteract each other. One improvement with decreasing the void count could be to apply tensioned peel ply when the winding is completed before curing it in room temperature.

The composites tubes were put in a freezer to lower the temperature so that the extraction would go easier, the difference in thermal expansion between the composite and HDPE mandrel makes the two separate from each other. This was done before the heat curing. There could be observed cracks on the outer epoxy layer on the composite tubes, but

after the heat curing the cracks looks to have healed itself. Worth noting is that it was only cracks on the surface that could be observed, whether cracks in or between layers occurred could not be determined.

The heat curing introduces a stress induction on the SFRP composite as the thermal expansion between the resin and the steel fiber is different. This will have some effects on both the SFRP ring samples and the hybrid ring samples.

6.2 Split-disk Test

The results from the split-disk testing, when considering the UTS between the three different fiber material configurations used, agreed with what could be expected. It shows that the CFRP ring specimens had an UTS of about four times higher than the SFRP ring samples, which corresponds with the UTS of carbon fiber being about four times higher than the 302A steel fiber. The hybrid ring samples showed an increased stress value of about 200MPa before the SFRP layers of the hybrid ring failed compared with the pure SFRP ring samples. This indicates that the hybridization between steel fiber and carbon fiber was successful in increasing the overall strength value of the composite first-ply-failure. After the SFRP layers failed in the hybrid ring samples the CFRP layers further picks up load while sporadically experience fiber failure while the extension propagates. The steel fiber layers broke across the width of the ring specimen located between the gap of the two half disk of the split-disk setup, while still maintaining strong bonding between the steel fiber- and carbon fiber layers on the opposite side of the fiber failure (180° of the failure). This could also be identified on the full SFRP ring samples, which indicates a very brittle failure, but also confirms a success in inducing failure to occur in the split region of the test setup.

The CFRP ring specimens strain-to-failure values corresponds to what could be expected when considering the carbon fibers material properties. The carbon fiber has a reported strain-to-failure of 1.8% and the split-disk test showed a similar value. The SFRP ring specimens stain-to-failure proved to have a much lower value than expected. The steel fiber used in this thesis, ASIS 302A, has a reported strain-to-failure of $\tilde{4}$% and fiber bundle tensile test indicates a strain-to-failure of 5%. The results from the split-disk test showed the SFRP ring samples to have a strain-to-failure at 1.16%, which is contradicting to what could be expected. The low strain-to-failure could also be identified in the SFRP part the hybrid ring specimens, were an even lower strain-to-failure of 1.01% could be observed. After the SFRP layers of the hybrid ring samples failed the ultimate failure occurred at a strain of 1.89%, which is reasonable as only the CFRP layers in the hybrid ring samples are left. Regarding the validity of the strain values it should be noted that obtaining accurate results are difficult, as many aspects of the split-disk test can obscure the results. The strain values are calculated as the extension over half the circumference of the ring samples, which becomes incorrect as the elongation as the test propagates causing the ring specimens to change its shape from a circle to more of an oval shape. Therefore the strain values sited in this thesis should be viewed with some reservation, and be used as a observational value when comparing the different composite configurations. As to why the

SFRP experienced such a low strain-to-failure than what could be expected is must likely a combination of

6.3 Impact and Burst Test

The pressure vessel that was impact tested showed matrix cracking that propagated out from the contact area. There could not be observed any cracks in the outer SFRP layer, which indicates to some degree that the ductility of the steel fiber was successfully in absorbing the impact load caused by the impactor. When comparing the impact results from [4] with the same impact load of 60J on pure CFRP pressure vessel there could be seen interfiber cracking at the area of contact.

The results from the burst testing on the pressure vessels, both impact damaged and "healthy", was inconclusive as the tightness of the seal was not adequate. The leak in the vessels occurred at 30bar and did not build up enough pressure to cause any failure in the composite part of the pressure vessels. There is difficult to identify the reason for the leak, but the problematic areas are often either insufficient tightness in the valves in the end domes, or due to improper sealing from the polyurethane liner that were injected inside the pressure vessels. This has been experienced from other projects that has produced the same type of pressure vessels as described in this thesis. Due to insufficient time there were not enough time to produce more pressure vessel for burst testing.

6.4 Mechanical Properties Result

The mechanical properties obtain through CLT and FEA are fairly similar, comparing these values with the mechanical values derived from the split-disk test there is a larger discrepancy. Were the experimental values are much lower than the analytical values.

When comparing the steel fiber composites with carbon fiber, there is a large difference in both weight and material used, where carbon fiber is superior. Carbon fiber costs around 6 times more than steel fiber. In comparison when using steel fiber to produce the composite pressure vessel, the steel fiber used in terms of material, the SFRP is 20 times heavier. Until the production price of steel fiber and improvements in strength is made, steel fiber will not be able to replace carbon fiber reinforced polymers. There is a need to further examine steel fiber material for use in composite overwrap in pressure vessels.

Chapter 7

Conclusion

The main objective for this thesis has been to investigated the hybridisation effect between steel- and carbon fiber when used in fiber reinforced polymer composite pressure vessels produced by filament winding method. From the literature study, steel fiber is a fiber material which has not been researched to a high degree, therefor this study have investigated various parameters that influences the mechanical properties when used as reinforcement fiber in composite. This has been achieved by experimental testing of produced composite products described in this thesis.

The experience from production of the composite products can be concluded as:

- Using steel fiber as reinforcement material when producing composites through filament winding method has proven to be successful, both as products in form of tubes and pressure vessel.

- Adequate bonding between steel fiber and epoxy matrix were achieved, with fiber volume fraction of 45% and small degree of voids. Hybridization between steel- and carbon fiber reinforced composite layers were achieved with strong bonding between layers.

- Stress concentration during heat curing of composite products containing steel fiber needs to be addressed by using epoxy resin that cures at lower .

- Steel fiber has a tendency to split during filament winding with high pre-tension on fiber.

The results from the experimental tests in this thesis can be concluded as:

- The results from the split-disk test showed that the composite ring specimens containing steel fiber (SFRP and hybrid) achieve a low strain-to-failure value (ϵ_f=1.1%), and did align with the results that was achieved when conducting dry fiber bundle tensile testing (ϵ_f=4-5%). When compared to the values of the carbon fiber com-

posite ring specimens (ϵ_f=1.8%), the steel fiber specimens experience a lower strain value. The results from the split-disk tests also show that the hybrid samples failed at a lower strain value than the pure SFRP samples.

- The hybridization achieved an increase in hoop tensile strength by improving the first-ply-failure of the hybrid ring samples with 1̃50MPa compared with the SFRP ring samples.

- The impact resilience of the outer layer of the composite overwrap in the pressure vessel showed to be improved with steel fiber as fiber reinforcement. When comparing the damage from the impact testing between the SFRP overwrap and CFRP overwrap, the SFRP had a more ductile response to the impact with far less fiber failure than what could be seen on the CFRP.

- The mechanical properties obtain through CLT and FEA are fairly similar, comparing these values with the mechanical values derived from the split-disk test there is a larger discrepancy. Were the experimental values are much lower than the analytical values.

Bibliography

[1] William F. Hosford. *Mechanical Behavior of Materials 2nd Edition*. Cambridge University Press, New York, 2010.

[2] Technical Data Sheet. Epikote resin mgs rimr 135 and epikure curing agent mgs rimh 134 rimh 137, August 2006. Momentive Specialty Chemicals Inc.

[3] ASTM International. ASTM D2290-19 Standard test method for apparent hoop tensile strength of plastic or reinforced plastic pipe. Technical report, West Conshohocken, PA, 2019. URL `https://compass.astm.org/EDIT/html_annot.cgi?D2290+19`.

[4] Erik Saeter, Kaspar Lasn, Fabien Nony, and Andreas T. Echtermeyer. Embedded optical fibres for monitoring pressurization and impact of filament wound cylinders. *Composite Structures*, 210:608 – 617, 2019. ISSN 0263-8223. doi: https://doi.org/10.1016/j.compstruct.2018.11.051. URL `http://www.sciencedirect.com/science/article/pii/S0263822318325662`.

[5] M. G. Callens. *Development of ductile stainless steel fibre components*. PhD thesis, Groep Wetenschap & Technologie, KU Leuven, 2014.

[6] D. Tran. Producing steel fiber reinforced polymer composite pipes. Master's thesis, Norwegian University of Science and Technology, Trondheim, 2016.

[7] M. G. Callens, L. Gorbatikh, E. Bertels, B. Goderis, M. Smet, and I. Verpoest. Tensile behaviour of stainless steel fibre/epoxy composites with modified adhesion. *Composites Part A: Applied Science and Manufacturing*, 69:208 – 218, 2015. URL `http://www.sciencedirect.com/science/article/pii/S1359835X1400373X`.

[8] Composites World. The markets: Pressure vessels (2018), 2018. URL `https://www.compositesworld.com/articles/the-markets-pressure-vessels-2016`.

[9] T.Q. Hua, R.K. Ahluwalia, J.-K. Peng, M. Kromer, S. Lasher, K. McKenney, K. Law, and J. Sinha. Technical assessment of compressed hydrogen storage tank systems for automotive applications. *International Journal of Hydrogen Energy*, 36(4):3037–3049, 2011.

[10] C. O'Brien, A. McBride, A. E. Zaghi, K. A. Burke, and A. Hill. Mechanical behavior of stainless steel fiber-reinforced composites exposed to accelerated corrosion. *Materials*, 10(7):772, 2017.

[11] E.J. Barbero. *Introduction to Composite Materials Design*. Composite Materials. CRC Press, 2010. ISBN 9781439894132. URL `https://books.google.no/books?id=pRfSBQAAQBAJ`.

[12] Y. Mosleh, D. Clemens, L. Gorbatikh, I. Verpoest, and A. W. van Vuure. Penetration impact resistance of novel tough steel fibre-reinforced polymer composites. *Journal of Reinforced Plastics and Composites*, 34(8):624–635, 2015. URL `https://doi.org/10.1177/0731684415574538`.

[13] S. T. Peters. Netting analysis of cylindrical pressure vessels, 2001. URL `http://www.process-research.com/Netting.pdf`.

[14] N. P. Vedvik. Essential mechanics of composites, 2014.

[15] Lindberg & Lund, 2019. URL `https://lindberg-lund.no/2018/06/08/synthene-hpe-elastomer-rt/`.

[16] Cell Profiler, 2019. URL `https://cellprofiler.org/`.

[17] D. Cohen. Influence of filament winding parameters on composite vessel quality and strength. *Composites Part A: Applied Science and Manufacturing*, 28(12):1035 – 1047, 1997. ISSN 1359-835X. doi: https://doi.org/10.1016/S1359-835X(97)00073-0. URL `http://www.sciencedirect.com/science/article/pii/S1359835X97000730`.

Appendix

Appendix A

Image Analysis

To find the fiber volume fraction there were conducted a image analysis. This approach started with preparing a cross section of the composite of interest that could be looked upon through a microscope. The microscope used to produce the images was a lecia MeF4 microscope. When high enough quality of the images of the cross section was taken they were analysed in program called Cell Porfiler. Cell Profiler provides a method to calculate the area of fibers vs the area of epoxy in the image. With enough tweaking of parameters on how cell profiler shall define the contours of the fiber it gives out a relatively accurate fiber volume fraction. the content of this appendix will contain the setup of Cell Profiler and the images it analysed.

# of accepted objects	175
10th pctile diameter	29.5 pixels
Median diameter	45.9 pixels
90th pctile diameter	72.3 pixels
Area covered by objects	67.8 %
Thresholding filter size	1.0
Threshold	0.465
Declumping smoothing filter size	13.4
Maxima suppression size	14.0

Magnification: 50 x

50 µm
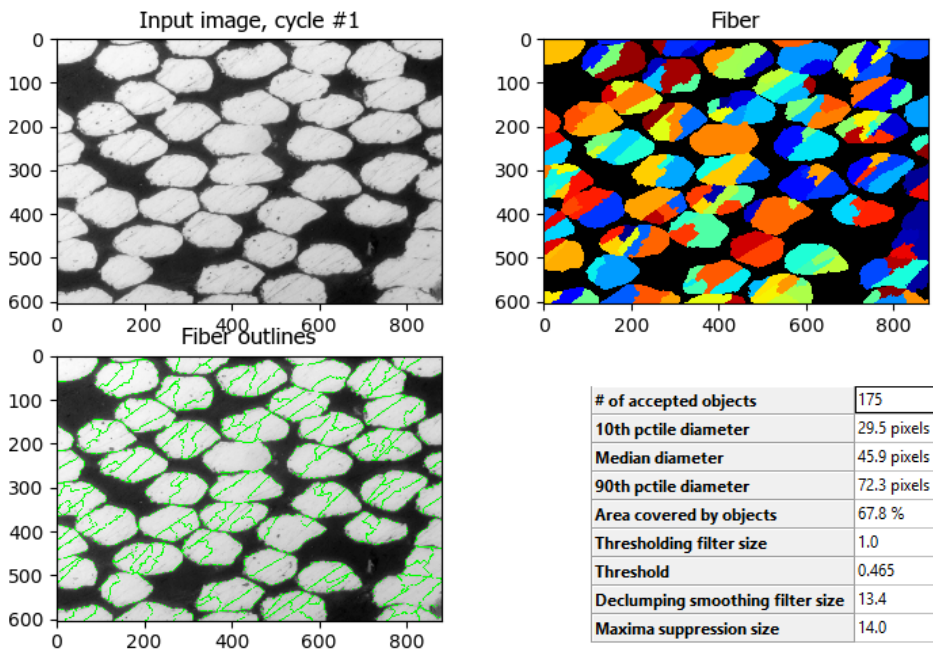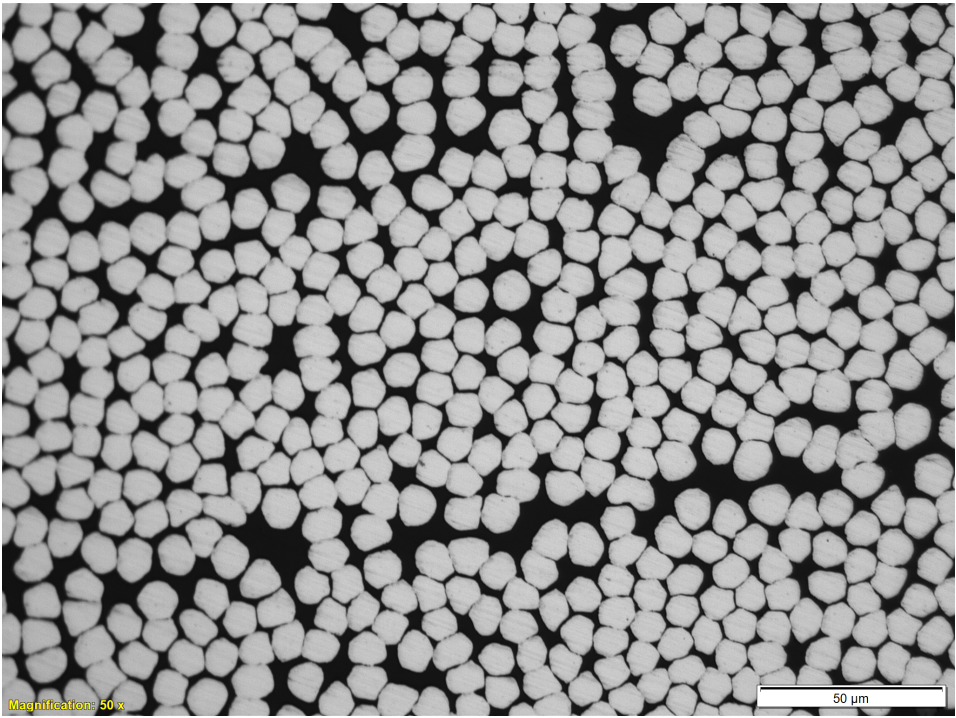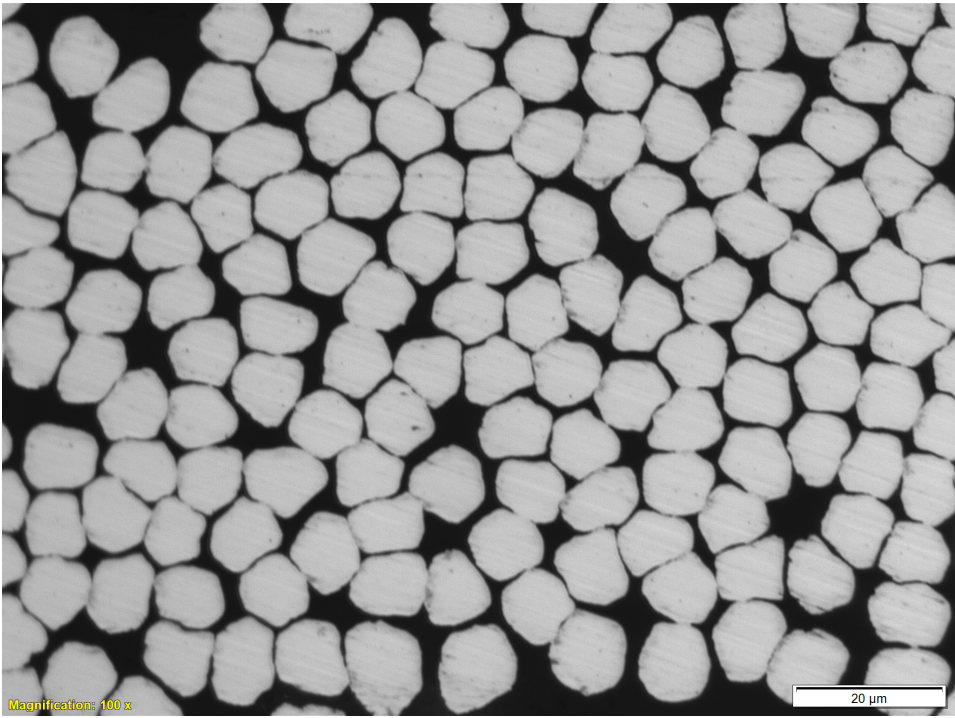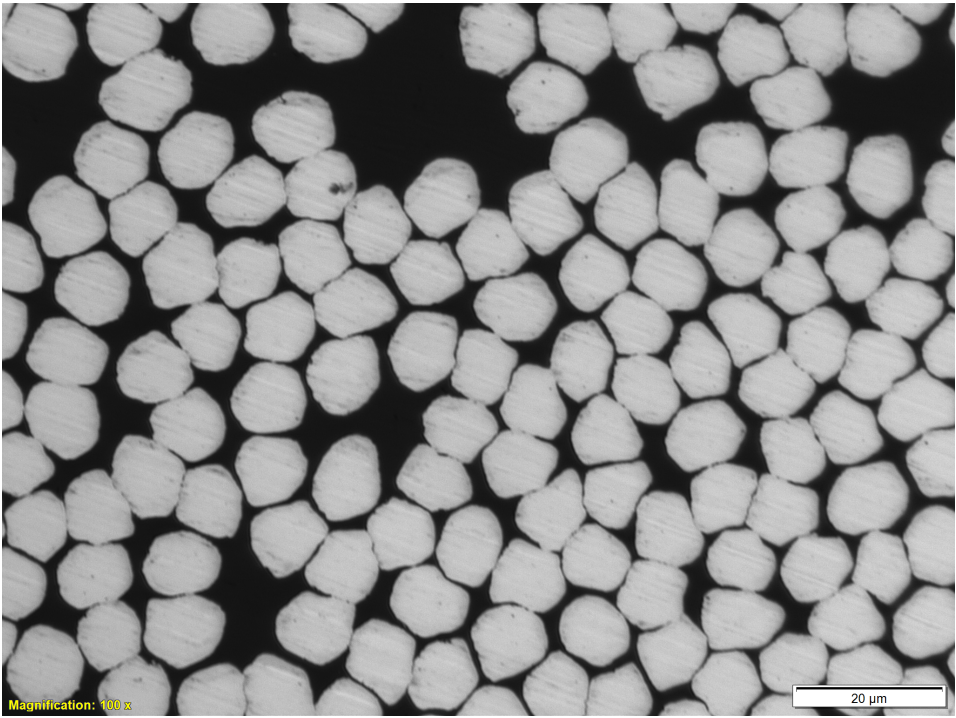
Appendix B

Ultrasound

As mentioned in the main text the ultrasound NDT investigation was decided not to further investigate, but the process and setup of the machine will be detailed here in case of interest to further look into it. The ultrasonic machine is of the type Olympus. Its main purpose in the NDT field is thickness measurements. The thickness measurements was tested on the SFRP ring specimens. This feature gave accurate reading on the steel and epoxy combination. The configuration was using the 2mm probe attachment and the setup on the Olympus was m222 P, which stands for plastic readings.

Appendix C

7.0.1   Risk Assesment

Sikkerhets- og kvalitetsgjennomgang av laboratorietester og verkstedsarbeid

Safety and Quality Evaluation of Activities in the Laboratory and Workshop

1 Identifikasjon - *Identification*

Dokumentnr. – *Document no.***:**

Kundenavn – *Customer name* Thomas Juell	Prosjektnavn – *Project name* Development of steel/carbon fiber reinforced polymer composite pressure vessel	Projektnr. – *Project no.* 70702300
Beskrivelse av arbeid – *Description of job* *Filament vikling, bearbeiding av prøver, testing av prøver*		Dato – *Date* *03-02-19*

2 Projekt - *Team*

Prosjektleder og organisasjon – *Project manager and organisation*	Thomas Juell	Ansvarlig for instrumentering – *Responsible for instrumentation.*	TJ
Leiestedsansvarlig – *Laboratory responsible*	TJ	Operatør – *Operator*	TJ
Auditør for sikkerhets og kvalitetsgjennomgang – *Auditer for safety check*	Carl Magnus Midtbø	Ansvarlig for styring av forsøk – *Responsible for running the experiment.*	TJ
Ansvarlig for eksperimentelt faglig innhold – *Responsible for experimental and scientific content*	TJ	Ansvarlig for logging av forsøksdata – *Responsible for logging and storing experimental data*	TJ
Ansvarlig for dimensjonering av last og trykkpåkjente komponenter – *Reponsible for dimensioning load bearing and pressurized components*	TJ	Ansvarlig for montering av testrigg – *Responsible for building the rig*	TJ

3 Viktig!! – *Important!!*

J: Ja – *Yes* / N: Nei - *No*

Er arbeidsordren signert? – *Is the work order signed?*	J
Har operatøren nødvendig kurs/trening i bruk av utstyret? - *Has the operator the required courses/training on the equipment?*	J
Har operatøren sikkerhetskurs? (påbudt) – *Has the operator followed the safety courses? (mandatory)*	J
Kan jobben gjøres alene? - *Can the work be done alone?*	J

- Dersom ja, er det med visse forbehold (for eksempel, må bruke alarm, ha avtale med noen som kommer innom med jevne mellomrom eller lignende). Dette må vurderes i Seksjon 5.*If yes, the work may have to be done under special conditions (e. g. must use the alarm, have agreement with somebody coming back periodically or similar). This shall be evaluated in Section 5.*

Må en ekspert se på oppstart av eksperimentet? Does an expert have to check the start of the experiment?	N

- Dersom ja, hvem? *If yes, who?*

4.1 Sikkerhet – *Safety* (Testen medfører – *The test contains*)

J: Ja – *Yes* / N: Nei - *No*

Stor last – *Big loads*	N	Brannfare – *Danger of fire*	J
Tunge løft – *Heavy lifting*	N	Arbeid i høyden – *Working at heights*	N
Hengende last – *Hanging load*	J	Hydraulisk trykk – *Hydraulic pressure*	J
Gasstrykk – *Gas pressure*	N	Vanntrykk – *Water pressure*	J
Høy temperatur – *High temperature*	N	Lav temperatur – *Low temperature*	N
Deler i høy hastighet – *Parts at high velocity*	J	Farlige kjemikalier – *Dangerous chemicals*	J
Sprutakselerasjon ved brudd – *Sudden acceleration at fracture/failure*	J	Forspente komponenter – *Pre-tensioned components*	J
Farlig støv – *Dangerous dust*	J	Kraftig støy – *Severe noise*	N
Klemfare – *Danger of pinching*	J	Roterende deler – *Rotating parts*	J

4.2 Påkrevet verneustyr – *Required safety equipment*

J: Ja – *Yes* / N: Nei - *No*

Briller (påbudt) – *Glasses (mandatory)*	J	Vernesko – *Safety shoes*	N
Hjelm – *Helmet*	N	Hansker – *Gloves*	J
Skjerm – *Screen*	J	Visir – *Visir*	N
Hørselsvern – *Ear protection*	J	Løfteredskap – *Lifting equipment*	J
Yrkessele, fallsele, etc. – *Harness ropes, other measures to prevent falling down.*	N		

Sikkerhets- og kvalitetsgjennomgang av laboratorietester og verkstedsarbeid

NTNU
Perleporten

5.1 Beskrivelse av aktivitet – *Description of the activity (see Appendix)*

Vurdering skal være basert på en skriftlig prosedyre for bruk av maskinen. I enkelte tilfeller kan prosedyre bli beskrevet direkte i tabellen nedenfor.

The evaluation shall be based on a written operating procedure for the machine. For simple cases the procedure can be directly described in the tables below.

Nr.	Beskrivelse av aktivitet – *Description of activity*	Fare – *Danger*	Lov, forskrift o.l. – *Legal requirements*	Prosedyre nr. – *Procedure no.*	Sannsynlighet – *Probability*	Konsekvens – *Consequence*	Risiko – *Risk*
1	Blanding av resin	Eksponering av hud	NTNU-HMS	1	3	A	3A
2	Blanding av resin	Exothermic reaksjon	NTNU-HMS	2	2	C	2C
3	Vikling	Klemfare av kroppsdeler, bli fanget av roterende deler	NTNU-HMS	3	3	B	3B
4	Bruk av båndsag	Kuttskade	NTNU-HMS	4	3	C	3C
5	Split-disk testing	Skade på kropp	NTNU-HMS	5	2	C	2C
6	Burst testing	Skade på kropp	NTNU-HMS	6	2	C	2C
7	Impact testing	Klemfare	NTNU-HMS	7	2	C	2C

5.2 Korrigerende Tiltak – *Corrective Actions*

Nr.	Korrigerende tiltak – Corrective action	Sannsynlighet – *Probability*	Konsekvens – *Consequence*	Risiko – *Risk*	Utført dato – *Date of action*
1	Bruke dobbelt hanske, være obs på at man kan ha våt resin på hanske. Bruke vernebriller	2	A	2A	28-02-19
2	Mikse resin i eget blandekabinett. Sørge for å tømme resin bøtte hvis full etter bruk.	1	A	1A	28-02-19
3	Være obs på håndplassering, ikke ha løst hengende plagg under vikling.	1	A	1A	28-02-19
4	Holde avstand fra blad under saging.	2	B	2B	28-02-19
5	Bruke verneskjold under tesing. Bruke vernebriller og hørselsvern	1	A	1A	28-02-19
6	Lukke alle åpne luker så godt som mulig, bruke ballast på luke rett over trykktanken. Bruke vernebriller og hørselsvern	1	B	1B	28-02-19
7	Være obs på håndplassering under testing. Bruke vernebriller og hørselsvern.	1	A	1A	28-02-19

Sikkerhets og kvalitetsgjennomgang av laboratorietester og verkstedsarbeid

NTNU
Perleporten

Sjekkliste: Er følgende feilkilder vurdert? – Check list: Is the following considered?   J: Ja – *Yes* / N: Nei - *No*

Tap av strøm – *Loss of electricity*	J	Overspenning – *Voltage surge*	N
Elektromagnetisk støy – *Electromagnetic noise*	N	Manglende aggregatkapasitet av hydraulikk – *Insufficient power of the machine*	N
Jordfeil – *Electrical earth failure*	N	Vannsprut – *Water jet*	N
Ustabilt trykk av hydraulikk/kraft – *Unstable pressure or hydraulic force*	N	Tilfeldig avbrudd av hydraulikk/kraft – *Unintended interruption of power supply*	J
Last-/ forskyvnings grenser etablert ? – *Are load and displacement limits established?*	J	Lekkasjer (slanger/koblinger, etc.) – *Leakage of pipes, hoses, joints, etc.*	J
Mulige påvirkninger fra andre aktiviteter – *Possible interference from other activities*	J	Mulige påvirkninger på andre aktiviteter – *Possible interference towards other activities*	N
Problemer med datalogging og lagring – *Troubles in loading and storage*	N	Brann i laboratoriet – *Fire in the laboratory*	J

6 Kalibreringsstatus for utstyr – *Calibration of equipment*
(ex: load cell, extensometer, pressure transducer, etc)

I.D.	Utstyr - *Equipment*	Gyldig til (dato) – *Valid until (date)*

7 Sporbarhet – *Tracebility*

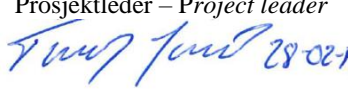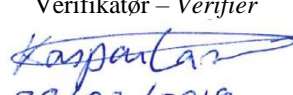| Eksisterer – Is there	J: Ja – *Yes* / N: Nei - *No*
Er alle prøvematerialene kjente og identifiserbare? – *Are all experimental materials known and traceable?*	J
Eksisterer det en plan for markering av alle prøvene? – *Is there a plan for marking all specimens?*	J
Er dataloggingsutstyret identifisert? – *Is the data aquisition equipment identified?*	J
Er originaldata lagret uten modifikasjon? – *Are the original data stored safely without modification?*	J
Eksisterer det en backup-prosedyre? – *Is there a back-up procedure for the data (hard disk crash)?*	N
Eksisterer det en plan for lagring av prøvestykker etter testing? – *Is there a plan for storing samples after testing?*	J
Eksisterer en plan for avhending av gamle prøvestykker? – *Is there a plan for disposing of old samples?*	J

8 Kommentarer – *Comments*

9 Signaturer – *Signatures*
Godkjent (dato/sign) – Approved (date/signature)

Prosjektleder – P*roject leader*	Verifikatør – *Verifier*	Godkjent – *Approved by*
[signature]	*Kaspartar* 28/02/2019	*[signature]* 05/4/2019

Sikkerhets og kvalitetsgjennomgang av laboratorietester og verkstedsarbeid

◼ NTNU
Perleporten

APPENDIX Bakgrunn - Background

Sannsynlighet vurderes etter følgende kriterier:
Probability shall be evaluated using the following criteria:

Svært liten Very unlikely 1	Liten Unlikely 2	Middels Probable 3	Stor Very Probable 4	Svært stor Nearly certain 5
1 gang/50 år eller sjeldnere – *Once per 50 years or less*	1 gang/10 år eller sjeldnere – *Once per 10 years or less*	1 gang/år eller sjeldnere – *Once a year or less*	1 gang/måned eller sjeldnere – *Once a month or less*	Skjer ukentlig – *Once a week*

Konsekvens vurderes etter følgende kriterier:
Consequence shall be evaluated using the following criteria:

Gradering – *Grading*	Menneske – *Human*	Ytre miljø, Vann, jord og luft – *Environment*	Øk/materiell – *Financial/Material*	Omdømme – *Reputation*
E **Svært Alvorlig** – *Very critical*	Død – Death	Svært langvarig og ikke reversibel skade – *Very prolonged, non-reversible damage*	Drifts- eller aktivitetsstans >1 år. – *Shutdown of work >1 year.*	Troverdighet og respekt betydelig og varig svekket – *Trustworthiness and respect are severely reduced for a long time.*
D **Alvorlig** – *Critical*	Alvorlig personskade. Mulig uførhet. – *May produce fatality/ies*	Langvarig skade. Lang restitusjonstid – *Prolonged damage. Long recovery time.*	Driftsstans > ½ år Aktivitetsstans i opp til 1 år – *Shutdown of work 0,5-1 year.*	Troverdighet og respekt betydelig svekket – *Trustworthiness and respect are severely reduced.*
C **Moderat** – *Dangerous*	Alvorlig personskade. – *Permanent injury, may produce serious health damage/sickness*	Mindre skade og lang restitusjonstid – *Minor damage. Long recovery time*	Drifts- eller aktivitetsstans < 1 mnd – *Shutdown of work < 1 month.*	Troverdighet og respekt svekket – *Troverdighet og respekt svekket.*
B **Liten** – *Relatively safe*	Skade som krever medisinsk behandling – *Injury that requires medical treatment*	Mindre skade og kort restitusjonstid – *Minor damage. Short recovery time*	Drifts- eller aktivitetsstans < 1uke – *Shutdown of work < 1 week.*	Negativ påvirkning på troverdighet og respekt – *Negative influence on trustworthiness and respect.*
A **Siker** - **Safe**	Injury that requires first aid	Insignificant damage. Short recovery time	Shutdown of work < 1day	

Risikoverdi = Sannsynlighet X Konsekvenser
Beregn risikoverdi for menneske. IPM vurderer selv om de i tillegg beregner risikoverdi for ytre miljø, økonomie/ material og omdømme. I så fall beregnes disse hver for seg.

Risk = Probability X Consequence
Calculate risk level for humans. IPM shall evaluate itself if it shall calculate in addition risk for the environment, economic/material and reputation. If so, the risks shall be calculated separately.

Rev. 10 – Aug 2018   Page 4 of 7

Risikomatrisen
Risk Matrix

I risikomatrisen er ulike grader av risiko merket med rød, gul eller grønn:

Rød: Uakseptabel risiko. Tiltak skal gjennomføres for å redusere riskoen.

Gul: Vurderingsområde. Tiltak skal vurderes.

Grønn: Akseptabel risiko. Tiltak kan vurderes ut fra andre hensyn.

Når risikoverdien havner på rødt felt, skal altså enheten gjennomføre tiltak for å redusere riskoen. Etter at tiltak er iverksatt, skal dere foreta ny risikovurdering for å se om riskoen har sunket til akseptabelt nivå.

For å få oversikt over samlet risiko: Skriv risikoverdi og aktivitetens IDnr. i risikomatrise (docx) / risikomatrise (odt). Eksempel: Aktivitet med IDnr. 1 har fått risikoverdi 3D. I felt 3D i risikomatrisen skriver du IDnr. 1. Gjør likedan for alle aktiviteter som har fått en risikoverdi. En annen måte å skaffe oversikt på, er å fargelegge feltet med risikoverdien i skjemaet for risikovurdering. Dette tydeliggjør og gir samlet oversikt over riskoforholdene. Ledelse og brukere får slik et godt bilde av risikoforhold og hva som må prioriteres.

In the risk matrix different degrees of risk are marked with red, yellow or green;

Red: Unacceptable risk. Measures shall be taken to reduce the risk.

Yellow: Assessment Area . Measures to be considered.

Green: Acceptable risk. Measures can be evaluated based on other considerations.

When a risk value is red, the unit shall implement measures to reduce risk. After the action is taken, you will make a new risk assessment to see if the risk has decreased to acceptable levels.

To get an overview of the overall risk: Write the risk value and the task ID no . the risk matrix (docx) / risk matrix (odt) . Example : Activity with ID no . 1 has been risk value 3D. In the field of 3D risk matrix type ID no . 1 Do the same for all activities that have been a risk . Another way to get an overview is to color the field of risk value in the form of risk assessment . This clarifies and gives overview of the risk factors . Management and users get such a good picture of the risks and what needs to be prioritized.

KONSEKVENS	Svært alvorlig	E1	E2	E3	E4	E5
	Alvorlig	D1	D2	D3	D4	D5
	Moderat	C1	C2	C3	C4	C5
	Liten	B1	B2	B3	B4	B5
	Svært liten	A1	A2	A3	A4	A5
		Svært liten	Liten	Middels	Stor	Svært stor
		SANNSYNLIGHET				

Prinsipp over akseptkriterium. Forklaring av fargene som er brukt i risikomatrisen.

Farge		Beskrivelse
Rød		Uakseptabel risiko. Tiltak skal gjennomføres for å redusere risikoen.
Gul		Vurderingsområde. Tiltak skal vurderes.
Grønn		Akseptabel risiko. Tiltak kan vurderes ut fra andre hensyn.

Til Kolonnen "Korrigerende Tiltak":

Tiltak kan påvirke både sannsynlighet og konsekvens. Prioriter tiltak som kan forhindre at hendelsen inntreffer, dvs sannsynlighetsreduserende tiltak foran skjerpende beredskap, dvs konsekvensreduserende tiltak.

For Column "Corrective Actions"

Corrections can influence both probability and consequence. Prioritize actions that can prevent an event from happening.

Oppfølging:

Tiltak fra risikovurderingen skal følges opp gjennom en handlingsplan med ansvarlige personer og tidsfrister.

Follow Up

Actions from the risk evaluation shall be followed through by an action plan with responsible persons and time limits.

Etterarbeid #

- Gå gjennom aktiviteten/prosessen på nytt.
- Foreta eventuell ny befaring av aktiviteten/prosessen for enten a) å få bekreftet at risikoverdiene er akseptable eller b) for å justere risikoverdiene.
- Gå gjennom, vurder og prioriter tiltak for å forebygge uønskede hendelser. Først skal dere prioritere tiltak som reduserer sannsynlighet for risiko. Dernest skal dere ta for dere tiltak som reduserer risiko for konsekvenser.
- Tiltakene skal føres inn i handlingsplanen. Skriv fristen for å gjennomføre tiltaket (dato, ikke tidsrom) og navn på den / de som har ansvar for tiltakene.
- Foreta helhetsvurdering for å avgjøre om det nå er akseptabel risiko.
- Ferdig risikovurdering danner grunnlag for å utarbeide lokale retningslinjer og HMS-dokumenter, opplæring og valg av sikkerhetsutstyr.
- Ferdig risikovurdering og eventuelle nye retningslinjer gjøres kjent/tilgjengelig for alle involverte.
- Sett eventuelt opp kostnadsoverslag over planlagte tiltak.